

## Best practice guide for the use of static and dynamic gas standards at monitoring stations including the evaluation of measurement uncertainty

### DELIVERABLE D5

Maitane Iturrate-Garcia<sup>1</sup>, Nicolas Sobanski<sup>2</sup>, Annika Kuß<sup>3</sup>, Robert Holla<sup>3</sup>, Dagmar Kubistin<sup>3</sup>, Naomi Farren<sup>4</sup>, Sivan Van Aswegen<sup>5</sup>, David Worton<sup>5</sup>, John Casey<sup>6</sup>, Paul Johnston<sup>6</sup>, Timothy Baker<sup>6</sup>, Laura Buchanan<sup>6</sup>, Louise Mittal<sup>6</sup>, Gary Fuller<sup>6</sup>, Tatiana Macé<sup>7</sup>, Karri Saarnio<sup>8</sup>

1 METAS; 2 Empa; 3 DWD; 4 UOY; 5 NPL; 6 KCL; 7 LNE; 8 IL

# EMPIR



This project has received funding from the EMPIR programme co-financed by the Participating States and from the European Union's Horizon 2020 research and innovation programme.

For more details about the Metrology for Nitrogen Dioxide project please visit

<http://empir.npl.co.uk/metno2/>

# 1 Table of Contents

Acronyms/Glossary .....	2
About deliverable D5 .....	3
1 Introduction .....	4
1.1 Background .....	4
1.2 NO <sub>2</sub> monitoring .....	4
2 Measurement results .....	6
2.1 Comparison 1 – A2.3.1 and A2.3.3 outputs .....	6
2.2 Comparison 2 – A2.3.2 outputs .....	40
2.3 Comparison 3 – A2.3.4 outputs .....	52
3 Recommendations .....	56
3.1 Measuring method .....	56
3.2 Calibration method .....	57
3.3 Evaluation of measurement uncertainty .....	59
References .....	61

## Acronyms/Glossary

CAPS: Cavity Attenuated Phase Shift

CEAS: Cavity Enhanced Spectroscopy

CLD: Chemiluminescence Detector

CRDS: Cavity Ring Down Spectroscopy

DQO: Data Quality Objectives

EEA: European Environment Agency

ETC/ACM: European Topic Centre on Air pollution and Climate change Mitigation

EMPIR: European Metrology Programme for Innovation and Research

EURAMET: European Association of National Metrology Institutes

GPT: Gas Phase Titration

HNO<sub>3</sub>: Nitric acid

ISO: International Organization for Standardization

LAQN: London Air Quality Network

LIF: Laser Induced Fluorescence

LOPAP: Long Path Absorption Photometry

LSO: Local Site Operators

MetNO<sub>2</sub>: Metrology for nitrogen dioxide

NABEL: Nationalen Beobachtungsnetz für Luftremdstoffe

NO: Nitrous Oxide

NO<sub>2</sub>: Nitrogen Dioxide

NO<sub>x</sub>: Nitrogen Oxides

NO<sub>y</sub>: Oxidised odd-nitrogen species

O<sub>3</sub>: Ozone

QCLAS: Quantum Cascade Laser Absorption Spectroscopy

QEPAS: Quartz-Enhance Photoacoustic Spectroscopy

WMO-GAW: World Meteorological Organization-Global Atmosphere Watch programme

## About deliverable D5

Deliverable D5 describes a series of guidelines on the use of static and dynamic gas mixture standards for the calibration of field instrumentation including the evaluation of measurement methods and uncertainty.

D5 is a best practice guide based on tests, experiments and a field based side-by-side comparison performed in Task 2.3 – "Assessment of data quality with direct calibration of ambient NO<sub>2</sub> measurements using new reference standards in air quality monitoring networks"– of the project MetNO<sub>2</sub> .

The guide is divided in 3 sections:

- Section 1 provides a brief description of ambient NO<sub>2</sub> measurements, including analytical methods and reference gas standards.
- Section 2 includes the results of the tests, experiments and side-by-side comparison performed.
- Section 3 comprises recommendations for the use of static and dynamic gas standards at monitoring stations.

This guide aims to provide guidance to improve the accuracy and comparability of the nitrogen dioxide (NO<sub>2</sub>) measurements performed at monitoring stations by direct instrument calibration with NO<sub>2</sub> reference standards. Furthermore, the evaluation of measurement uncertainties contributes to the quantification of the offset caused by non-specific instruments (i.e. how complete is the conversion of NO into NO<sub>2</sub> for subsequent measurements).

The guide is oriented to sites of air quality monitoring programmes measuring NO<sub>2</sub> and/or atmospheric monitoring programmes collecting NO<sub>2</sub> data for air quality models.

# 1 Introduction

## 1.1 Background

NO<sub>2</sub> is a toxic gas that has implications for air quality, atmospheric chemistry and climate change. NO<sub>2</sub> plays a key role in ozone and secondary particle formation (Lai et al., 2013), influences the oxidative capacity of the atmosphere and significantly contributes to air pollution (Villena et al., 2012). Atmospheric NO<sub>2</sub> emissions come from natural and anthropogenic sources (Richter et al., 2005; Robinson and Robbins, 1970). Industrial boiler and traffic, especially diesel fuelled vehicles, are the main anthropogenic sources (Carslaw and Beevers, 2004; Lerda et al., 2000). High ambient amount fractions of NO<sub>2</sub> and long-term exposure have direct impact on public health, causing inflammation of the airways, cardiovascular diseases and premature mortality among others (Bernard et al. 2001; Latza et al., 2009; Stieb et al. 2016; WHO, 2013).

NO<sub>2</sub> is considered an essential climate variable by the Global Climate Observing System (GCOS), because of its role as precursor for aerosols and ozone, that needs to be monitored on a global scale. In addition, as a result of NO<sub>2</sub> impact on air quality and public health, the European Union mandates legal limits for NO<sub>2</sub> amount fractions (Air Quality Directive 2008/50/EC) and sets upper limits for annual NO<sub>x</sub> emissions (National Emission Ceilings (NEC) Directive 2016/2284/EC). Despite these regulations, NO<sub>2</sub> ambient amount fractions has not decreased as expected (Casquero-Vera *et al.*, 2019); even in some European countries, this decrease has been slower than the decline in NO<sub>x</sub> emissions (EEA, 2019). These facts have led to an increasing research effort to understand NO<sub>2</sub> trends and their potential causes and, particularly, to improve the accuracy and comparability of NO<sub>2</sub> measurement data from monitoring sites.

## 1.2 NO<sub>2</sub> monitoring

In Europe, there are more than 3000 sites monitoring and reporting NO<sub>2</sub> data (Malley et al., 2018). These data together with air quality modelling (ETC/ACM, 2013) are used to identify long-term trends in NO<sub>2</sub> amount fractions, to evaluate emission inventories, to ensure legislative compliance and to evaluate the effectiveness of applied mitigation strategies (EEA, 2018). Furthermore, data and model outputs are used to give insight into anthropogenic NO<sub>2</sub> emission impacts on atmospheric chemistry. However, in order to accomplish these tasks, data are required to be accurate and comparable among stations. Gas measurement accuracy is strongly dependent on the analytical methods and quality of the calibration gases used at the monitoring stations.

### 1.2.1 Analytical methods

Due to the importance of NO<sub>2</sub> in air quality and climate change, several direct and indirect analytical methods to measure NO<sub>2</sub> have been developed over the past decades.

### *Indirect analytical methods*

The method most commonly used in monitoring sites is the chemiluminescence detection (CLD), recommended by the European legislation (European Standard, EN 14211, 2012) as reference method. In the indirect analytical method CLD (Ridley and Howlett, 1974), NO<sub>2</sub> is measured indirectly by the chemiluminescent reaction of NO with ozone. First, NO<sub>2</sub> is reduced to NO by using catalytic (i.e. heated molybdenum surface) or photolytic converters. Second, the light emission of the electronically excited NO<sub>2</sub> – a product generated in the reaction of ambient NO with ozone added to the air sample – is measured to estimate the NO amount fraction (Kley and McFarland, 1980). The NO<sub>2</sub> amount fraction is derived by subtraction of NO from the NO<sub>x</sub> signal. The main issues of this method are related to cross-sensitivity, low conversion efficiency (Ryerson *et al.*, 2000) and artefacts (Tuzson *et al.* 2013). The cross-sensitivity has been observed in catalytic and photolytic converters, when compounds other than NO<sub>2</sub> (i.e. oxidised nitrogen compounds NO<sub>y</sub>) are converted to NO (Dunlea *et al.*, 2007, Steinbacher *et al.*, 2007). This interference may lead to systematically overestimated NO<sub>2</sub> amount fractions.

### *Direct analytical methods*

More recently, the European rising concern on air quality together with the need of accurate NO<sub>2</sub> measurements have pushed research in developing and improving NO<sub>2</sub> selective analytical methods. These methods have addressed, partially or totally, the issues of the indirect methods associated to cross-sensitivity and efficiency of the NO<sub>2</sub> conversion to NO. Long path absorption photometry (LOPAP), laser induced fluorescence (LIF) and luminol chemiluminescence, among others, belong to this category of methods. Another promising technique for direct NO<sub>2</sub> measurements is laser spectroscopy. Laser spectroscopy includes methods such as quartz-enhance photoacoustic spectroscopy (QEPAS; Patimisco *et al.* 2014), direct absorption spectroscopy (McManus *et al.*, 2015), quantum cascade laser absorption spectroscopy (QCLAS; Sirtori and Nagle, 2003) and cavity ring-down spectroscopy (CRDS) and its related forms (cavity enhanced (CEAS) and attenuated phase shift spectroscopy (CAPS)) (Mazurenka *et al.*, 2005; Wada and Orr-Ewing, 2005). The advances in these methods highlight the urgent need to characterise and evaluate their applicability for long-term NO<sub>2</sub> measurements.

In this guide, we present results of measurements performed with CAPS, QCLAS and CLD.

### 1.2.2 Reference gas standards

Besides adequate selective methods, the use of reference gas standards to calibrate NO<sub>2</sub> analysers is essential to ensure accurate and comparable data among monitoring stations.

Reference gas standards are generated statically or dynamically. Static gas standards are produced following ISO 6142-1:2015. These standards, kept in pressurised cylinders, have limited lifetime depending on the components used and their amount fractions in the mixture. Dynamic gas standards are generated following ISO 6145-1:2019, by different methods such permeation and diffusion. Dynamic standards are used in applications that require low amount-of-substance fraction standards and/or reactive compounds.

Most monitoring stations, equipped with indirect instruments for measuring NO<sub>2</sub> (i.e. CLD), calibrate their instruments with diluted NO static gas standards and use gas phase titration of NO with ozone ( $\text{NO} + \text{O}_3 \rightarrow \text{NO}_2 + \text{O}_2 + \text{light}$ ) to measure the conversion efficiency for NO<sub>2</sub> of the instrument (Steinbacher et al., 2007). The increasing development of selective methods to measure NO<sub>2</sub> have highlighted the need of generating and using appropriate NO<sub>2</sub> reference gas standards at atmospherically relevant amount fractions (from few nmol/mol (10 – 50 nmol/mol) up to 500 nmol/mol). The uncertainty of these standards must also be low ( $\leq 1\%$ ) to comply with the Data Quality Objectives (DQOs) for NO<sub>2</sub> measurements established by the WMO-GAW program in its implementation plan 2013-2016 (WMO-GAW, 2017).

However, generating stable and accurate reference standards of NO<sub>2</sub> at low amount fractions is challenging due to the reactivity of NO<sub>2</sub>. Different impurities have been reported in both static and dynamic gas standards (Flores et al., 2012a; Flores et al., 2012b; Hughes et al., 1977), being HNO<sub>3</sub> the major impurity. In order to minimise the presence of these impurities, a deeper knowledge of the chemistry behind the impurity formation is essential. Also, identifying and quantifying impurities adequately together with the use of improved methods to prepare gas reference standards (e.g. use of treated surfaces) will contribute to improve the accuracy of the references. Further information about impurities and generation of static reference standards can be found on the following deliverables of the project MetNO<sub>2</sub>:

- Deliverable D1: "Best practice guide for the preparation of static primary NO<sub>2</sub> reference standards".
- Deliverable D3: "Description of the techniques for the determination of major impurities in NO<sub>2</sub> reference standards, with recommendations for impurity analysis and methods to suppress their formation".

Results from several comparison exercises – NO<sub>2</sub> static reference standards vs. traditional gas phase titration (GPT) and NO<sub>2</sub> dynamic reference standards vs. GPT – in terms of repeatability, accuracy and measurement uncertainty are included in this guide.

## 2 Measurement results

### 2.1 Comparison 1 – A2.3.1 and A2.3.3 outputs

In these activity (A2.3.1 and A2.3.3), effects of using the static NO<sub>2</sub> standards and traditional NO standards on data quality (i.e. repeatability and accuracy) were compared. For that purpose, a 1 mol/mol static NO<sub>2</sub> reference standard developed in the project (A1.1.3) was used at different quality monitoring sites to calibrate direct and indirect instruments (see

Table 1).



Table 1: List of partners, sites and instruments used in comparison 1

Partner	Number of instruments	Instrument type	Number of sites	Site	Site type
Empa	3	CAPS, CLD, QCLAS	1	Dübendorf NABEL (CH)	suburban
DWD	3	CAPS, CLD (2)	1	Hohenpeißenberg (DE)	rural
KCL	1	CLD	5	Belvedere, Bexley (BX2) Greatness Park, Sevenoaks (ZV1) Islington, Holloway Road (IS2) Islington, Arsenal (IS6) Elephant & Castle, Southwark (SK6)	suburban suburban urban urban urban

### 2.1.1 Empa results

This subsection presents the results of a side-by-side instrument inter-comparison in field conditions that took place at the Dübendorf NABEL suburban station. The inter-comparison involved the deployment of 3 different NO<sub>2</sub> calibration methods:

- dilution of a 1 µmol/mol NO<sub>2</sub> in N<sub>2</sub> standard from a 10 L cylinder (static direct method);
- gas phase titration of a 20 µmol/mol NO in N<sub>2</sub> standard from a 50 L cylinder (static indirect method);
- and reference gas mixtures generated by permeation using a NO<sub>2</sub> permeation tube calibrated in a magnetic suspension balance (dynamic direct method). Results from this calibration belongs to subsection 2.4 *Comparison 4 – A2.3.4 outputs*.

The three calibration methods were applied on four instruments: a molybdenum converter Chemiluminescence Detector (CLD), a Cavity Attenuated Phase Shift spectrometer (CAPS), a commercial Quantum Cascade Laser Absorption Spectrometer (MIRO) and a custom made one (MINAS).

#### 2.1.1.1 Experimental setup

##### Location

The CLD instrument was located in the air quality monitoring station in Dübendorf (main station), which belongs to the NABEL network, while the rest of instruments were located in an annex of the station. During the calibration phases, the CLD was connected to the common calibration line via a 5 m PFA pipe. For the ambient air measurements, the CAPS and the 2 QCLAS were sampling from the common inlet of the station annex, and the CLD from the main station inlet. Both inlets have exactly the same design, are horizontally separated by ≈ 10 m and sample from the same altitude; they are therefore considered collocated.

The instruments were calibrated in parallel with each of the three calibration methods (static direct, static indirect and dynamic direct methods). After the calibration, the instruments measured ambient air from the collocated inlets for two weeks (the instrument MIRO measured only for one week).

The NABEL network provided ancillary measurements of ambient O<sub>3</sub> and meteorological parameters during the comparison.

#### NO<sub>2</sub> instruments

The CLD instrument is a T200 NO/NO<sub>2</sub>/NO<sub>x</sub> analyser (Teledyne Technologies Inc.). It is the instrument employed permanently at the Dübendorf station of the NABEL network for regulatory ambient NO<sub>x</sub> measurements.

The CAPS is a NO<sub>2</sub> Analyser MODEL T500U (Teledyne Technologies Inc.).

MIRO and MINAS are both QCLAS based instruments. They both rely on the same concept. A Quantum Cascade Laser (QCL) is used as a laser light source. The laser beam is coupled into an astigmatic Herriott type multipass cell where the NO<sub>2</sub> containing gas sample is continuously flowing at ≈ 1 slm and 50 to 100 mbar. After multiple reflections between the astigmatic mirrors, the beam exits the cell and is directed onto an infrared detector. The light intensity received by the detector is directly linked to the amount fraction of NO<sub>2</sub> in the gas sample. The MIRO instrument uses a NO<sub>2</sub> absorption line at 1630 cm<sup>-1</sup>, and the MINAS instrument a line at 1599 cm<sup>-1</sup>.

#### Calibration methods

A NO<sub>2</sub> in N<sub>2</sub> 10 L cylinder with a nominal amount fraction of 1.0006 μmol/mol, provided by project partner VSL, was used as a static direct standard (abbreviated as "Cyl" calibration). The content of this cylinder was diluted by NO<sub>2</sub> free synthetic air ([NO<sub>2</sub>] < 50 pmol/mol, Messer Group) to reduce the amount fraction to a relevant range (from 0 to ≈ 100 nmol/mol). The 1 μmol/mol NO<sub>2</sub> air flow was controlled by a SilcoNert2000 coated MFC (range 0 - 500 sccm, Vögtlin Instruments GmbH). The dilution air flow was controlled by a second MFC (range 0 - 10 slm, Vögtlin Instruments GmbH), both calibrated against a traceable Molbox system (Fluke Calibration). During the whole calibration phase, the dilution flow was kept constant at 5 slm, and the 1 μmol/mol NO<sub>2</sub> flow was varied stepwise between 0 and 500 sccm (total flow varied from ≈ 5 to 5.5 slm). An overflow of minimum 1 slm was located 2 m downstream of the mixing point to ensure constant pressure at the inlet of the NO<sub>2</sub> instruments. These ones had their inlet located 2 to 6 m downstream of the overflow. For the different amount fractions, the stabilization time was ≈ 30 min.

The gas phase titration calibration (static indirect method, abbreviated as "GPT" calibration) was carried out using a NO in N<sub>2</sub> 20 μmol/mol 50 L cylinder from NPL as a NO standard. The GPT reaction itself took place in a commercial GPT unit (BREITFUSS Messtechnik GmbH, model MKAL-GPTM), which includes an O<sub>3</sub> lamp, a NO + O<sub>3</sub> reactor, and a dilution system. The dilution gas was the same as for the Cyl calibration. The output of this unit was connected in place of the dilution T-piece used for the Cyl calibration to ensure comparability and cancel the effect of the calibration line. The total flow was kept constant at 5 slm, the NO flow was kept constant at 40 sccm. Different NO<sub>2</sub> amount fractions were obtained by changing the light intensity of the O<sub>3</sub> lamp.

As a dynamic direct standard, a portable generator based on permeation and dilution (ReGaS1) provided by METAS was used. Together with the portable generator, a permeation tube with a permeation rate of 605 ng/min at 40°C was used. The permeation tube was previously calibrated by METAS using their magnetic suspension balance (primary standard). To generate NO<sub>2</sub> reference gas

standards, the permeation tube was introduced in the oven chamber of the generator and different flows set to generate the desired amount fraction range. The meta-parameters set for the calibration are given in Table 2. The set amount fraction ranged from 20 to 65 nmol/mol with a total flow ranging from 4.5 to 5.3 slm (with 1 or 2 dilution steps), from which at least 0.5 slm was overflowing. As for the GPT calibration, the instrument was connected in place of the dilution T-piece used for the Cyl calibration to ensure comparability and cancel the effect of the calibration line. Due to the lack of zero point (0 nmol/mol) of the generator, the instrument offset was obtained by sampling directly from a synthetic air gas cylinder. The carrier and dilution gas was the same NO<sub>2</sub> free synthetic air as for the Cyl calibration.

Table 2: ReGaS calibration meta-parameters

Oven temperature	Oven pressure	Oven carrier flow	Dilution flow	Dilution steps
41.6°C	2.6 bar	300 sccm	3 to 6 slm	1 and 2

### 2.1.1.2 Calibration data

#### Stabilization period

To ensure stable signals, the output of the calibration setups were monitored with the instrument MINAS prior to the calibration phase. For the Cyl calibration, the output was monitored for  $\approx$  3 hours (Figure 1). For the GPT calibration, the stabilization phase prior to the calibration was done at  $\approx$  130 nmol/mol (Figure 2). For the ReGaS calibration, a total output flow of 3 slm with a set amount fraction of  $\approx$  105 nmol/mol was measured.

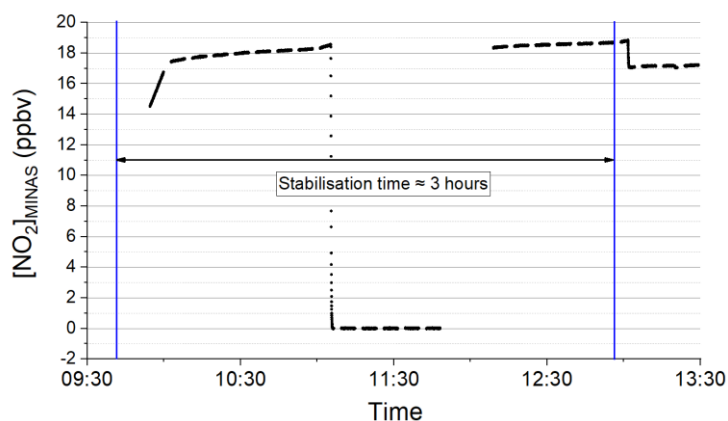


Figure 1: Cyl calibration stabilization phase

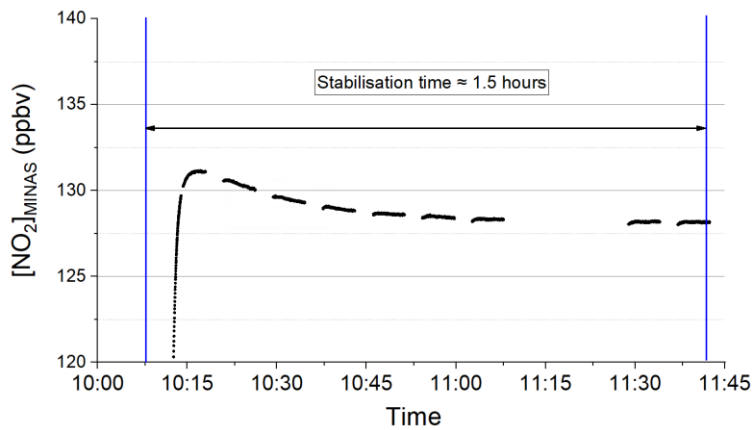


Figure 2: GPT calibration stabilization phase

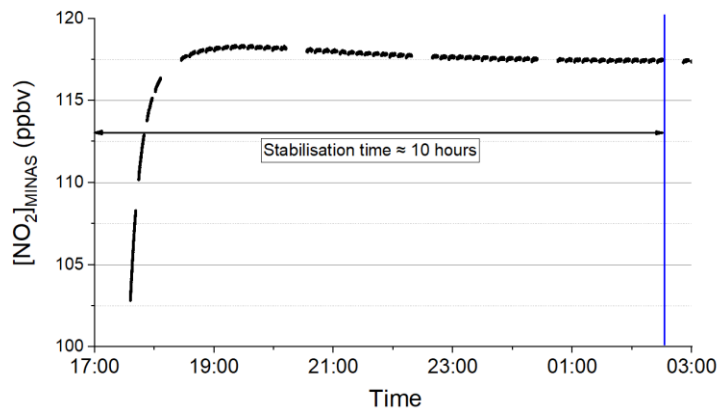


Figure 3: ReGaS calibration stabilization phase

Figure 1 – Figure 3Figure 27 show that among the 3 calibration methods, the GPT is the method that requires the shortest stabilization time, while the ReGaS demands the longest stabilization time. This is likely due to the fact that for the GPT method, once  $\text{NO}_2$  is formed from the reaction between  $\text{NO}$  and  $\text{O}_3$ , the sample only gets in contact with PFA of the tubing, whereas for the Cyl and ReGaS calibrations, the  $\text{NO}_2$  circulates through MFCs and valves that include stainless steel elements. These elements, even when coated (SilcoNert 2000), might be less inert to  $\text{NO}_2$  than PFA, thus increasing the stabilization time. Furthermore, in the case of ReGaS calibration, most of this time (10 hours) is due to the stabilization period of the permeation unit (i.e. time needed by the membrane of the permeation unit to give a stable permeation rate at certain temperature).

### Parallel calibration

The calibration curves for the four instruments and the three different methods obtained prior to the ambient air measurements are shown in Figure 4–Figure 6. The datasets were linearly fitted using the least square method. On each of these three plots, the X-axis represents the span (calculated amount fraction) and the Y-axis the value measured by each of the instrument. For the Cyl calibration (Figure 4), the span  $[\text{NO}_2]$  is obtained from the dilution factor and the bottle amount

fraction. For the ReGaS calibration (Figure 5), the device software automatically calculates the span amount fraction, based on the permeation rate of the permeation unit and the internal dilution factors. For the GPT calibration (Figure 6), the span  $[\text{NO}_2]$  is obtained from the difference of  $[\text{NO}]$  measured by the CLD without and with adding different amounts of  $\text{O}_3$ . The original calibration factors of the four instruments – that is, the calibration/parameters that yielded the values on the Y-axis – are given in Table 3. The error bars on the X and Y-axis represent the  $2\sigma$  standard deviation. For the X-axis, this corresponds to the propagation of the MFC standard deviations for the Cyl calibration, to the standard deviation on the output amount fraction for the ReGaS, and to the propagated standard deviation of the  $[\text{NO}]$  measurement for the GPT calibration. The black lines represent 0.9, 1 and 1.1 slope.

Table 3: Original calibration for the four  $\text{NO}_2$  instruments

Instrument	Reference/Original calibration
MINAS	HITRAN spectral database
MIRO	HORIBA APML 370M ( $\text{NO}_2$ permeation)
CAPS	HORIBA APML 370M ( $\text{NO}_2$ permeation)
CLD	NABEL GPT procedure

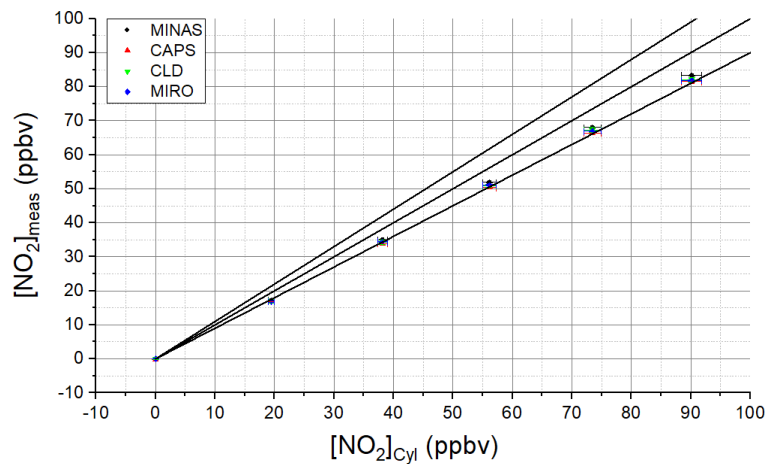


Figure 4: Cyl calibration curve

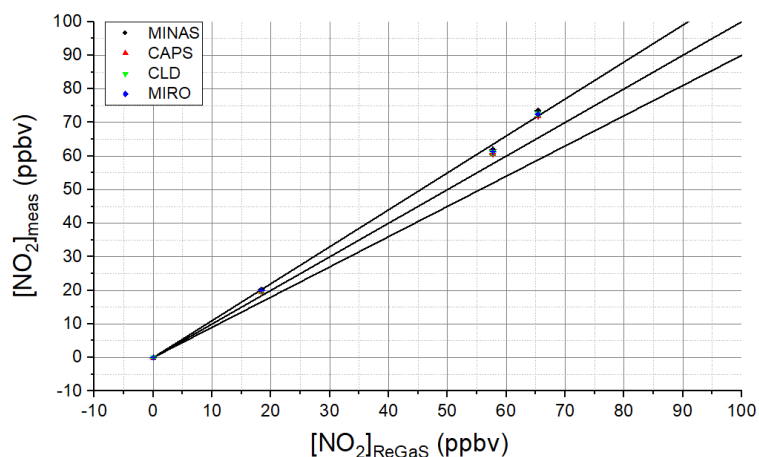


Figure 5: ReGaS calibration curve

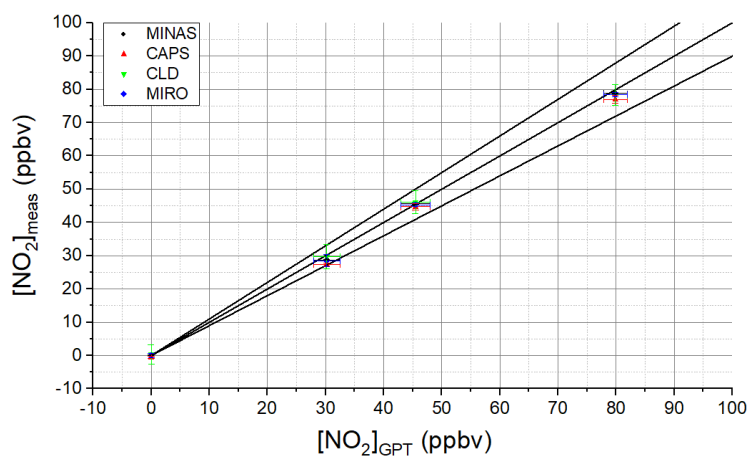


Figure 6: GPT calibration curve

Overall, the instruments show very similar calibration factors (offset and slope) for a given calibration method, however, the slopes vary by up to 10% for a single instrument depending on the calibration procedure. The slope and the intercept of the calibration curves are shown in Figure 7. The error bars represent the total uncertainty of the calibration factors, including the uncertainty of the NO cylinder amount fraction and NO instrument (CLD) for the GPT calibration, the NO<sub>2</sub> cylinder and the MFCs for the Cyl calibration and the uncertainty on the calculated span [NO<sub>2</sub>] for the ReGaS. The points circled with a continuous line correspond to the Cyl calibration, the dotted line corresponds to the GPT and the dashed line represents the ReGaS data. The largest discrepancies are found between the Cyl and ReGaS calibration, with differences in slopes values of around 20%, which cannot be explained by uncertainties.

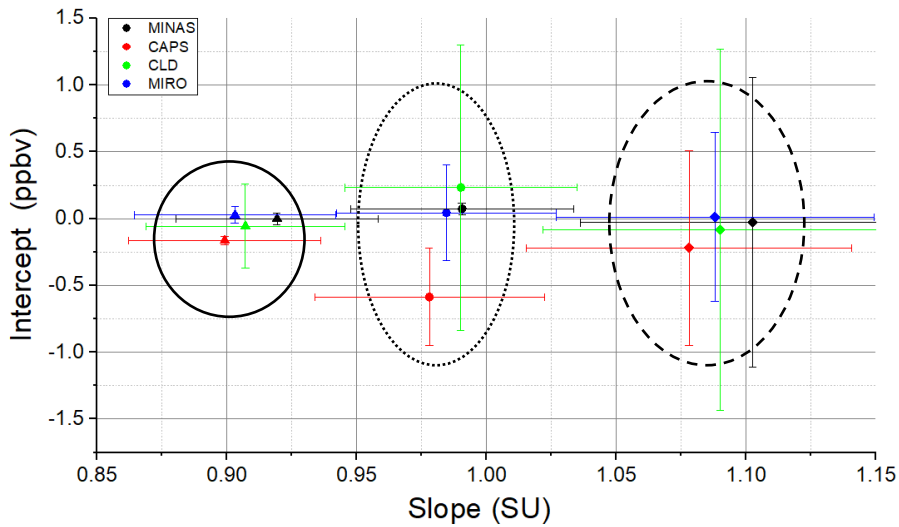


Figure 7: Intercepts and slopes corresponding to the linear fit of the data in Figure 4 –Figure 6. The points circled with a continuous line correspond to the Cyl calibration, the dotted line corresponds to the GPT calibration and the dashed line represents the ReGaS calibration data

#### Pre vs post ambient measurement calibration

After the ambient measurement period (see subsection 2.1.1.3 *Ambient air measurements*), the CAPS and CLD devices were recalibrated with the Cyl and GPT methods. The comparison between the pre and post ambient measurements calibration factors are shown in Figure 8. The slopes of the pre and post calibrations agree well within the uncertainties (max deviation = 1 %). However, the intercept values for the CAPS do not agree, which is likely due to drifts in the zero of the instrument.

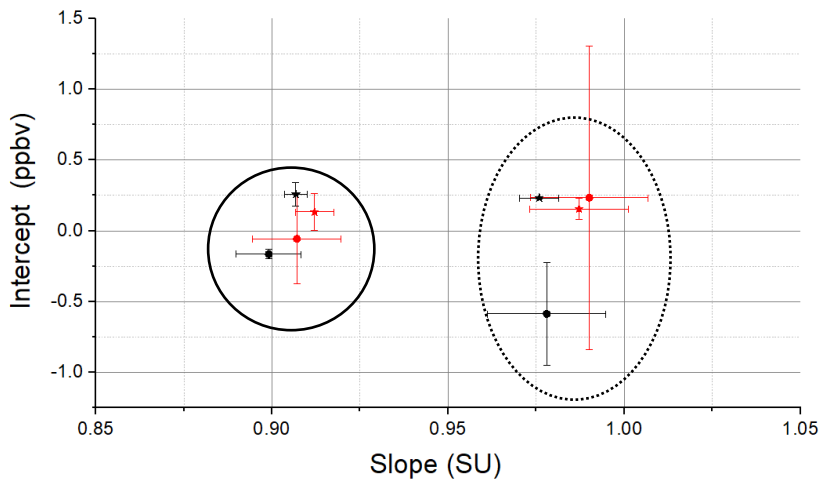


Figure 8: Intercept and slope of the pre and post ambient measurement calibrations. The pre calibration parameters are represented by points, and the post calibration parameters by stars. The CAPS data are in black and the CLD data are in red. The points circled with a continuous line correspond to the Cyl calibration, the dotted line corresponds to the GPT.

### 2.1.1.3 Ambient air measurements

#### Corrections of ambient air data

Several corrections were applied to the different ambient NO<sub>2</sub> datasets. As the aim of this work is to investigate uncertainties arising from the different calibration methods, final data are presented with uncertainties of the calibration methods only (therefore not accounting for the additional uncertainties from the different corrections). The CLD data were only corrected for drifts according to the internal correction procedure of the NABEL network (Technischer Bericht zum Nationalen Beobachtungsnetz für Luftfremdstoffe (NABEL) 2018) to ensure representativity of the data quality.

#### • Drifts

After each calibration sequence presented above, a 2 points calibration was performed (at 0 and 40 nmol/mol) using a HORIBA APML 370M permeation device on the MIRO and CAPS instruments. A similar calibration was repeated every day during the entire measurement period. This was used to account for drifts. Figure 9 shows the offset and scaling factor drifts for the two instruments calibrated daily.

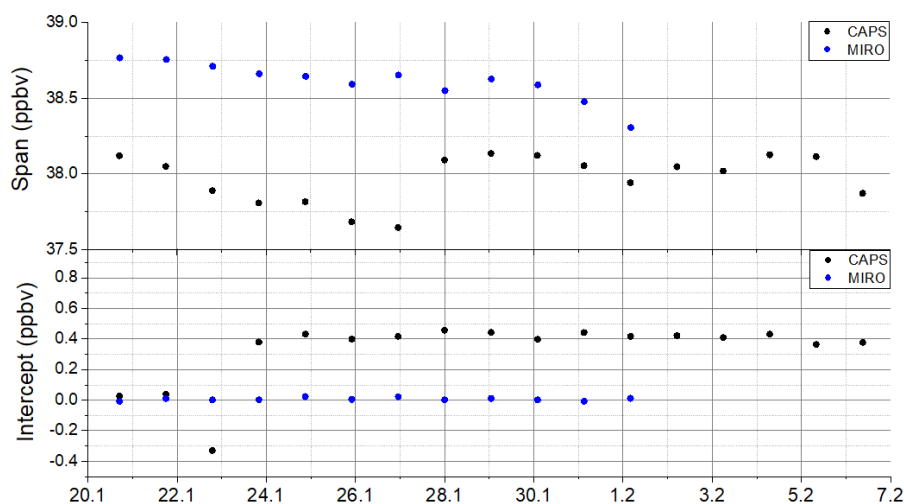


Figure 9: Intercept and span drifts of the CAPS and MIRO devices

#### • NO + O<sub>3</sub> reaction in the sampling line

As the comparison took place in a suburban environment, high amount fractions of NO and O<sub>3</sub> were observed. Significant amounts of NO<sub>2</sub> could therefore be formed in the tubing of the inlet lines from the O<sub>3</sub> + NO reaction. This bias was corrected by approximating the residence time in the different individual inlets (based on tubing volumes and flow rates) and using the IUPAC value for  $k_{O_3+NO}$ . The calculated NO<sub>2</sub> formed during sampling ranged from 0 up to 1.8 nmol/mol (maximum obtained for 5 seconds residence time (for the CLD device), 20 nmol/mol NO and 70 nmol/mol O<sub>3</sub>).

#### • Water interferences

Previous experiments on the two QCLAS instruments revealed no effect from water sampling. The CAPS instrument has an integrated dryer which was regenerated shortly before the measurement campaign, it is therefore assumed that interferences from water were negligible.



### Ambient air measurement overview

The  $\text{NO}_2$  mixing ratios obtained by the four instruments corrected with the Cyl calibration factors are shown in Figure 10 with a one-minute resolution.  $\text{NO}_2$  mixing ratios ranged from 0.5 to 60 nmol/mol during the measurement period, with high variability as expected at this site. A zoom on a high  $[\text{NO}_2]$  period (27/01/2020) and low  $[\text{NO}_2]$  measurement (28-29/01/2020) is shown in Figure 11. Over the whole range of mixing ratios, the MINAS and MIRO instruments show excellent agreements (blue and black lines on Figure 10 – Figure 11 nearly overlapping). The CAPS shows good agreement with the mid-IR instruments (MIRO and MINAS) at high  $[\text{NO}_2]$ , but has an offset at low  $[\text{NO}_2]$  of  $\approx 200$  pmol/mol. The CLD device shows a significant difference with the other instruments, from 1 nmol/mol at low mixing ratios up to 8 nmol/mol (obtained for the maximum measured  $\text{NO}_2$  of  $[\text{NO}_2]_{\text{MINAS}} = 49$  nmol/mol). This is typically attributed to interferences from other nitrogen oxides,  $\text{O}_3$  and  $\text{H}_2\text{O}$ .

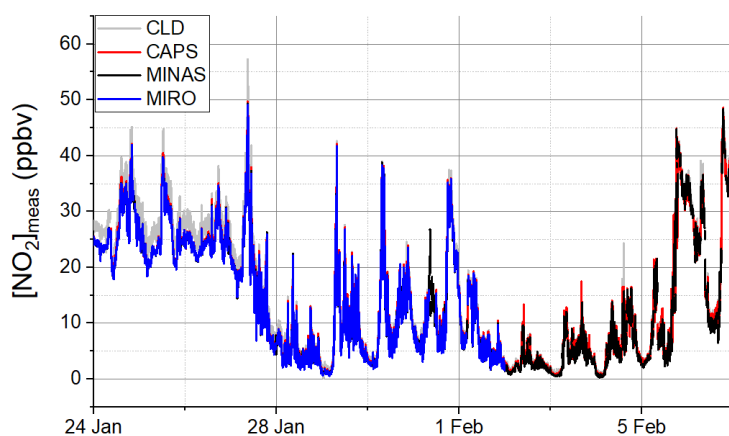


Figure 10: Ambient  $[\text{NO}_2]$  measured from the 24/01 to the 07/02/2020 at the Dübendorf NABEL station

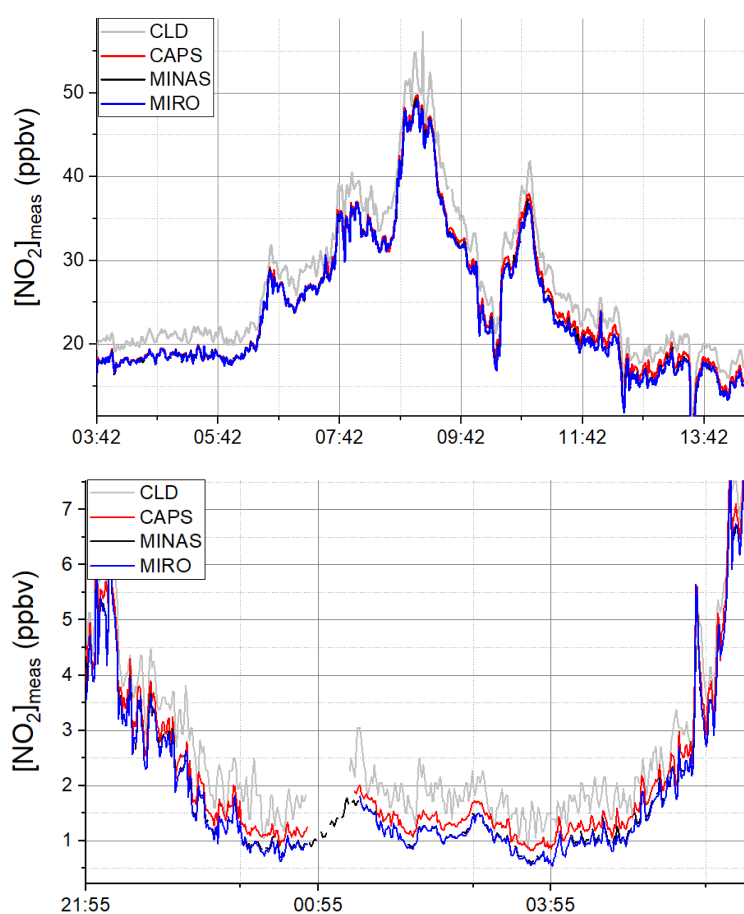


Figure 11: Example of high (top) and low [NO<sub>2</sub>] (bottom) mixing ratios measurements.

### Correlation between the different instruments

The correlation between MINAS (taken as a reference) and the three other instruments on the ambient air measurements is shown in Figure 12 –Figure 14. Each of those figure correspond to the data obtained with a given calibration method. The CLD shows the least agreement with MINAS, with a slope of  $\approx 1.06$ , regardless of the calibration method. The CAPS and mid-IR instruments show very good agreement with slopes comprised between 0.99 and 1.01. The best agreement is obtained between the two mid-IR instruments (MIRO and MINAS). Overall, correcting the instrument data with the GPT parameters yields the least agreement between MINAS and the two other direct detection instruments (MIRO and CAPS).

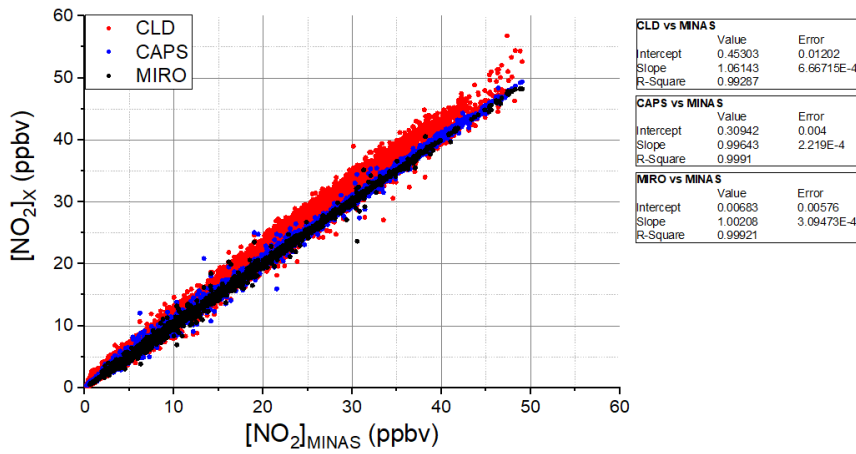


Figure 12: Correlation between MINAS and the three other instrument using ambient data obtained with the Cyl calibration parameters.

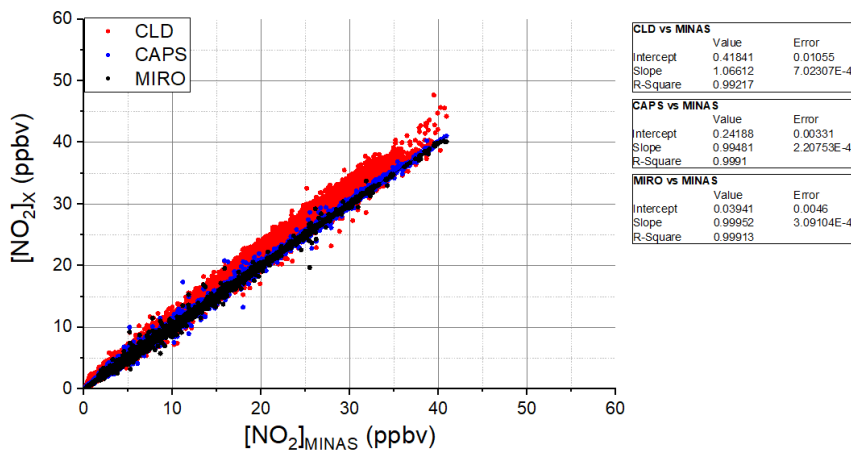


Figure 13: Correlation between MINAS and the three other instrument using ambient data obtained with the ReGaS calibration parameters.

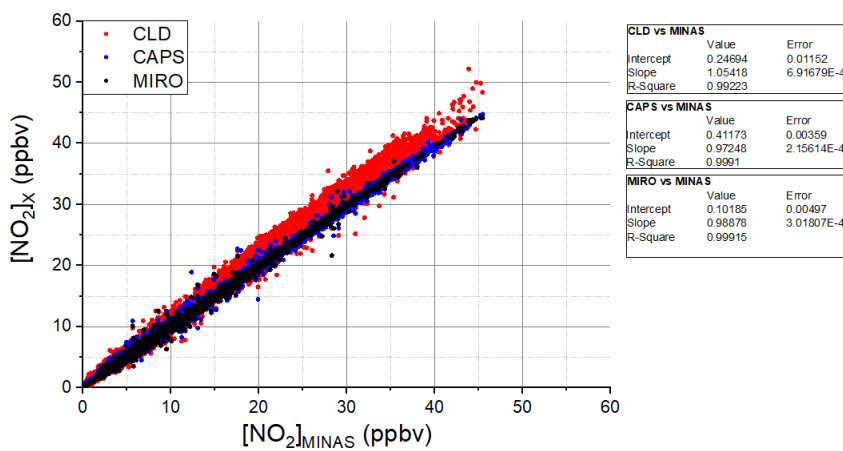


Figure 14: Correlation between MINAS and the three other instrument using ambient data obtained with the GPT calibration parameters.

## Measurement uncertainties

A box plot of the absolute uncertainties calculated for each  $[\text{NO}_2]$  data point with a one-minute resolution is shown in Figure 15.

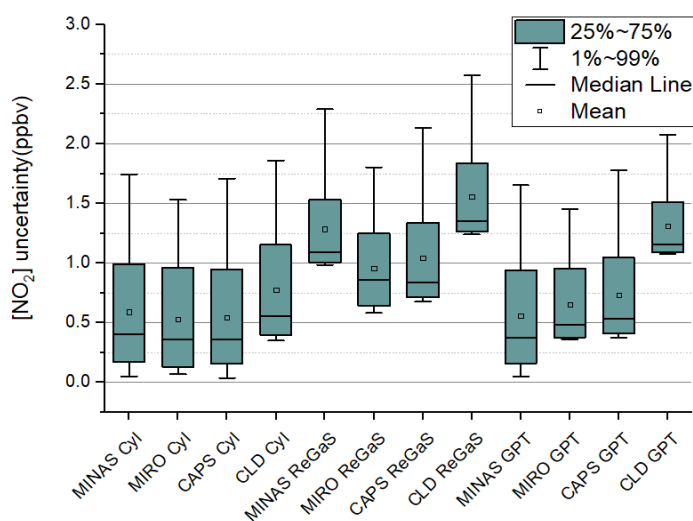


Figure 15: Box plot of the uncertainties on the ambient  $\text{NO}_2$  measurements.

The uncertainty data presented in the previous figure are a combination of the fit uncertainties of the calibration curves and the uncertainties of the standards (2k factor):  $\text{NO}_2$  amount fraction of the VSL cylinder (uncertainty = 4 %), ReGaS output amount fraction (uncertainty = 4.7 %), and NO amount fraction of the NPL cylinder (uncertainty = 1 %). Figure 16 shows a box plot of the ratio between the uncertainties of the standards and the total uncertainties for all ambient air  $[\text{NO}_2]$  measurements. This plot should be interpreted as follows: for the GPT calibration, the uncertainty of the NO amount fraction in the gas cylinder represents on average 10% of the total ambient  $[\text{NO}_2]$  measurement uncertainties. For the Cyl calibration, the uncertainty on the  $\text{NO}_2$  amount fraction in the  $\text{NO}_2$  cylinder represents on average 90% of the total uncertainty.

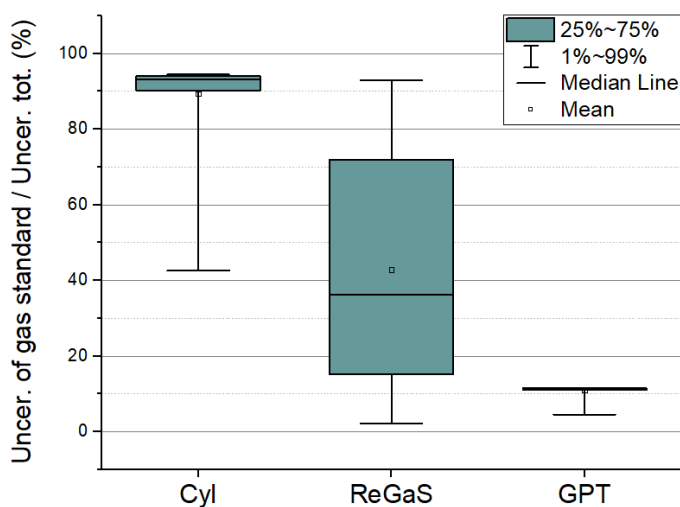


Figure 16: Share of the primary standard uncertainty in the total measurement uncertainty of ambient  $[\text{NO}_2]$

#### 2.1.1.4 Summary

This activity presents the results of ambient [NO<sub>2</sub>] measurements at a suburban NABEL station by four different instruments: a CLD, a CAPS and two QCLAS. Those four instruments were sequentially calibrated with three different methods: using a direct static standard (Cyl calibration), and indirect static standard (GPT calibration) and a dynamic standard (ReGaS calibration). The analysis of the calibration data shows that for a given method, the four instruments agree within a range of 2%. The ReGaS and Cyl calibration parameters differed significantly (up to 10%) compared to the GPT calibration, which is the currently established reference method.

The CAPS and the 2 QCLAS ambient [NO<sub>2</sub>] datasets are in very good agreements, with slopes ranging from 0.994 to 1.002 using the factors from the direct calibration methods (Cyl and ReGaS). The GPT calibration parameters yield the least agreement between those three instruments. Regardless of the calibration method used, the CLD data showed the least agreement with the three other instruments with slopes around 1.06.

Analysis of the uncertainty data showed that the lowest uncertainties are obtained with the Cyl and GPT calibrations and with the direct measurement instruments (CAPS, MIRO, MINAS). For the Cyl calibration method, the final ambient [NO<sub>2</sub>] measurement uncertainties are mostly limited by the relatively high uncertainty on the NO<sub>2</sub> amount fraction in the gas cylinder. For the GPT method, the uncertainty is limited by the uncertainty on the NO measurements used to derive the span amount fraction. For the ReGaS method, the situation lies in between the two other methods: the ReGaS calibration done in this work resulted in an instrument offset parameter fit with a high uncertainty on it causing the relatively big spread of the data in Figure 16.

### 2.1.2 DWD results

#### 2.1.2.1 Experimental setup

The National Physical Laboratory (NPL) provided a newly developed static reference standard for NO<sub>2</sub> (1 μmol/mol NO<sub>2</sub> in N<sub>2</sub>) to use at DWD monitoring station Hohenpeissenberg. The currently applied conventional calibration concept using gas phase titration of NO and O<sub>3</sub> was compared to the by NPL developed static reference standard for NO<sub>2</sub>.

Four calibration intercomparisons using two DWD NO<sub>2</sub> instruments based on different measurement principles (CLD and CAPS) were performed. A chemiluminescence instrument (ECO PHYSICS CLD 770 AL ppt) coupled with a photolytic converter (Blue Light Converter, Air Quality Design) was used to quantify NO and NO<sub>2</sub>. For direct NO<sub>2</sub> detection, a cavity attenuated phase shift NO<sub>2</sub> Monitor (CAPS, Aerodyne) was used. Unlike chemiluminescence-based monitors, this instrument requires no conversion of NO<sub>2</sub> to another species. Regular drift corrections were performed using NO<sub>2</sub>-free air (filtered pure air) for periodic automated baseline measurements every two hours.

### 2.1.2.2 Calibration data

#### Calibration with gas phase titration of NO

Four calibrations of the NO<sub>2</sub> instruments (CLD and CAPS) were performed during the two-week measurement period in July 2020 via the standard calibration procedure using gas phase titration. The multi-gas calibrator AirQrate (mlu-recordum, Environmental Monitoring Solutions) was applied for the routine standard calibration, which is operationally being used for weekly NO and NO<sub>2</sub> calibrations.

The calibration procedure is based on the dilution of a working standard NO gas mixture (10.21 µmol/mol ± 0.2 µmol/mol NO in N<sub>2</sub>, Air Liquide) and gas phase titration based on the reaction of O<sub>3</sub> with NO to NO<sub>2</sub>. The NO working standard is traceable to NPL (10.014 µmol/mol ± 0.04 µmol/mol NO in N<sub>2</sub>, NPL cylinder # 2795). This procedure includes background measurements with purified air (PAG 003 – Ion-Kat, Eco Physics), followed by a span NO volume mixing ratio of 31.745 nmol/mol and finally the titration of NO + O<sub>3</sub> → NO<sub>2</sub> + O<sub>2</sub>. Ozone is added to the NO in deficit. Therefore, the difference of NO measured with and without conversion by the CLD instrument can be used as a reference to calibrate the CAPS monitor.

The calibrations including the calibration factors are summarised in

Table 4. During all four calibrations, both instruments were calibrated simultaneously. The volume mixing ratio of NO<sub>2</sub> measured by the CLD instrument is determined from the difference of NO converted (NO.c) and the actual NO measured

$$NO_2 = \frac{(NO.c - NO)}{conv. efficiency}$$

and

$$conv. efficiency = 1 - \frac{NO.c(1) - NO.c(2)}{NO(1) - NO(2)}$$

with (1) denoting values before addition of ozone and (2) denoting values during addition of ozone.

The average conversion efficiency of the CLD instrument was  $73.58 \pm 0.56$  % and the average sensitivity of the CAPS monitor was  $0.987 \pm 0.002$  with a relative precision of 0.1%.

Table 4: CLD and CAPS NO<sub>2</sub> calibration via gas phase titration of NO + Ozone using the calibration unit AirQrate. NO mixing ratios before O<sub>3</sub> addition was 31.745 nmol/mol. The standard deviation of the single measured amount fractions are given in brackets.

Date of calibration	CLD			CAPS	
	remaining NO [nmol/mol]	NO <sub>2</sub> expected [nmol/mol]	conversion Efficiency [%]	NO <sub>2</sub> observed [nmol/mol]	cal.coeff. [nominal/signal]
13/07/2020	11.599 (0.037)	20.047 (0.013)	<b>0.737</b>	19.982 (0.024)	<b>0.997</b>
16/07/2020	11.607 (0.020)	20.073 (0.049)	<b>0.739</b>	19.662 (0.026)	<b>0.980</b>
21/07/2020	11.573 (0.015)	20.155 (0.008)	<b>0.741</b>	19.639 (0.027)	<b>0.974</b>
13/08/2020	11.218 (0.024)	20.515 (0.009)	<b>0.726</b>	20.359 (0.025)	<b>0.997</b>

#### Calibration with new NO<sub>2</sub> static reference standard

In addition to the standard calibration procedure (gas phase titration), four multi-point calibrations were performed with the newly developed NO<sub>2</sub> cylinder (NPL – S413, 1.03 μmol/mol ± 0.05 μmol/mol NO<sub>2</sub> in N<sub>2</sub>) during the two week period (see Table 5) . Two mass flow controllers (Zero air: 20 slm, Brooks® Instrument, NO<sub>2</sub>: 100 sccm, Brooks® Instrument, both stainless steel) were applied to generate NO<sub>2</sub> mixing ratios from 10 nmol/mol to 50 nmol/mol.

Table 5: Calibration of CAPS analyser with new static reference gas standard by NPL (cylinder # S413)

Date of calibration	Dilution Flow [synthetic air] [ml/min]	NPL S413 NO <sub>2</sub> Flow [ml/min]	Target NO <sub>2</sub> conc. (diluted) [nmol/mol]	CAPS NO <sub>2</sub> conc. (calibrated) [nmol/mol] (stdev)	Calibration Factor	Deviation [%]
13.07.2020	2058.79	100.41	46.50	35.165 (0.025)	<b>0.756</b>	-0.244
	2058.79	21.32	10.25	6.818 (0.009)	<b>0.665</b>	-0.335
	2058.79	83.39	38.93	29.384 (0.019)	<b>0.755</b>	-0.245
	2058.79	10.31	4.98	2.960 (0.014)	<b>0.594</b>	-0.406
	2058.79	41.16	19.60	14.343 (0.015)	<b>0.732</b>	-0.268
	2058.79	50.35	23.87	17.672 (0.013)	<b>0.740</b>	-0.260
14.07.2020	2058.79	83.39	38.93	29.783 (0.009)	<b>0.765</b>	-0.235
	2058.79	21.32	10.25	7.241 (0.015)	<b>0.706</b>	-0.294
	2058.79	100.41	46.50	36.292 (0.011)	<b>0.780</b>	-0.220
	2058.79	10.31	4.98	3.154 (0.009)	<b>0.633</b>	-0.367
15./16.07.2020	2058.79	41.34	19.69	14.605 (0.011)	<b>0.742</b>	-0.258
	2058.79	83.39	38.93	29.944 (0.017)	<b>0.715</b>	-0.231
	2058.79	21.32	10.25	6.831 (0.021)	<b>0.712</b>	-0.334
21.07.2020	2058.79	39.91	19.02	13.488 (0.017)	<b>0.716</b>	-0.291
	2058.79	62.23	29.34	21.363 (0.011)	<b>0.712</b>	-0.272
	2058.79	10.31	4.98	2.989 (0.017)	<b>0.723</b>	-0.400
	2058.79	100.41	46.50	35.372 (0.014)	<b>0.722</b>	-0.239
				Average:	<b>0.716</b>	-0.288



### 2.1.2.3 Comparison between calibration methods

Calibrations using NPL NO<sub>2</sub> cylinder were performed directly after the GPT calibrations. GPT calibration factors were applied to the CAPS instrument. The calibration comparison is shown in Table 6 and Figure 17.

Table 6: Summary of the comparison between the NO<sub>2</sub> static cylinder calibration and the gas phase titration method.

date of calibration	slope	intercept
13.07.2020	0.764	-0.808
14.07.2020	0.772	-0.854
15.07.2020	0.767	-0.481
21.07.2020	0.787	-1.174
<b>mean</b>	<b>0.772</b>	<b>-0.829</b>
<b>stdev</b>	<b>0.009</b>	<b>0.245</b>

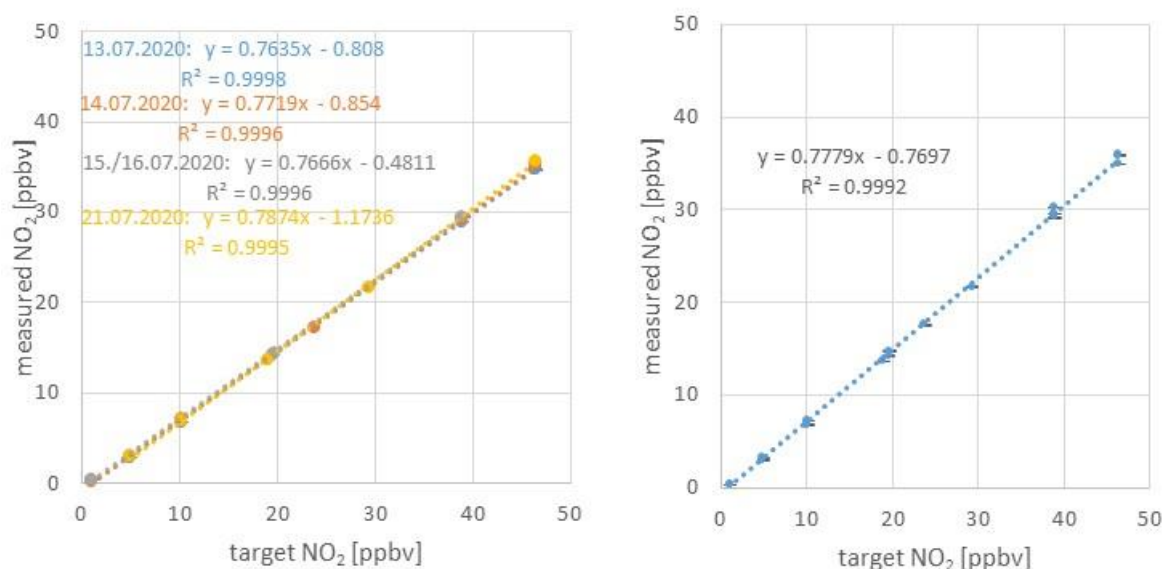


Figure 17: NPL - S413 (diluted NO<sub>2</sub> amount fraction - target) versus measured NO<sub>2</sub> amount fraction at CAPS Monitor (date of calibration: 2020-07-13 blue, 2020-07-14 orange, 2020-07-15/16 grey, 2020-07-21 yellow) (including linear fit); use of individual calibration factor of gas phase titration prior each multipoint NPL calibration

The targeted NO<sub>2</sub> amount fraction of the static reference standard is on average 23 % ( $\pm 3$  %) higher than the measured amount fraction on the CAPS instrument (Figure 18). Possible reasons for this deviation could be NO<sub>2</sub> absorption on stainless steel parts of the calibration unit (MFC, pressure reducer) and/or NO<sub>2</sub> loss on the cylinder walls over time. NO<sub>2</sub> losses on the MFC surface had been investigated by replacing the NO<sub>2</sub> MFC with a flow reducing orifice confirming the deviation of 23 %. NO<sub>2</sub> losses on the pressure reducer (stainless steel) have not been investigated as no suitable components (e.g. Silconert coated pressure reducer) were available. Recalibration of the NPL NO<sub>2</sub> cylinder will take place in the upcoming month to verify its initial amount fraction.

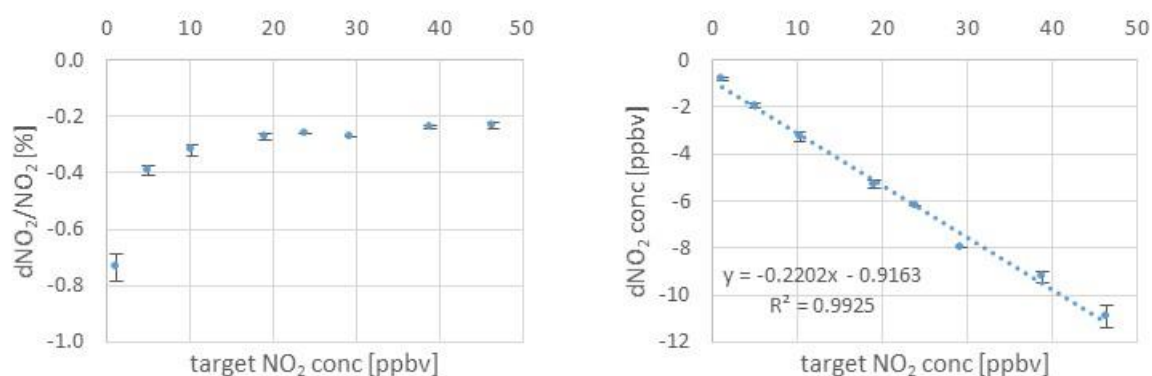


Figure 18: Relative deviation (left) and absolute deviation (right) of the measured NO<sub>2</sub> amount fractions detected on CAPS analyser from the targeted NO<sub>2</sub> amount fraction of the NPL static NO<sub>2</sub> standard (the error bar indicates the standard deviation of the sampled data)

#### 2.1.2.4 Uncertainty budget

The uncertainty budget of the two different calibration methods are calculated by the uncertainty of the MFCs ( $U(2\sigma) = 2.8\%$ ), the uncertainty of the NO cylinder amount fraction (Air Liquide NO  $U(2\sigma) = 2\%$ ), the reproducibility of the CLD NO<sub>2</sub> converter efficiency (1.52 %, determined from four consecutive calibrations) and the reproducibility of the CAPS sensitivity (1.2 %). These uncertainties propagate to an uncertainty of the measured NO<sub>2</sub> values of 3.8 % for the chemiluminescence detector and 4.5 % for the CAPS detector, when applying the GPT calibration method. For the NO<sub>2</sub> calibration using the new static reference standard generated by NPL (cylinder #S413 with a NO<sub>2</sub> amount fraction of  $1.03 \mu\text{mol/mol} \pm 0.05 \mu\text{mol/mol}$ ). The estimation of the uncertainty for the NO<sub>2</sub> measurement with the CAPS instrument is analogue to the calibration operating gas phase titration with NO and O<sub>3</sub> using the same uncertainties for the dilution system ( $U_{\text{MFC's}}(2\sigma) = 2.8\%$ ) and the uncertainty of the cylinder concentration (NPL  $U_{\text{NO}_2}(2\sigma) = 5\%$ ). These uncertainties propagate to an uncertainty of the measured NO<sub>2</sub> values of 5.8 % for the CAPS analyser. The precision of the CAPS analyser is in the order of 0.1 % negligible. The uncertainties for both calibration methods are summarised in **Error! Reference source not found.**

Table 7: relative Uncertainty ( $2\sigma$ ) of measured values on analysers (CLD and CAPS instrument)

Calibration method	CLD NO	CLD NO <sub>2</sub>	CAPS NO <sub>2</sub>
GPT	3.4 %	3.8 %	4.5 %
NO <sub>2</sub> static reference gas cylinder	n/a	n/a	5.8 %

### 2.1.3 KCL results

#### 2.1.3.1 Experimental setup

This subsection details the results of field tests on NO<sub>2</sub> calibration cylinders. These cylinders were manufactured to have amount fractions (approx. 1 µmol/mol) that can be used to calibrate ambient NO<sub>2</sub> instruments without dynamic dilution.

The stability of these cylinders was tested in field deployments at 2 suburban and 3 urban LAQN monitoring sites belonging to the London Air Quality Network (LAQN), which use chemiluminescent methods. King's / Imperial College London carried out the field tests.

Five zero and five NO<sub>2</sub> cylinders were deployed at air pollution measurement sites in London between 12<sup>th</sup> February 2020 and 10<sup>th</sup> September 2020.

NO<sub>2</sub> cylinders were used in conjunction with routine calibrations using NO in N<sub>2</sub> and zero air scrubbers.

The cylinders installed at London Air Quality Network (LAQN) monitoring site, ZV1 Sevenoaks - Greatness Park, are shown in Figure 19.

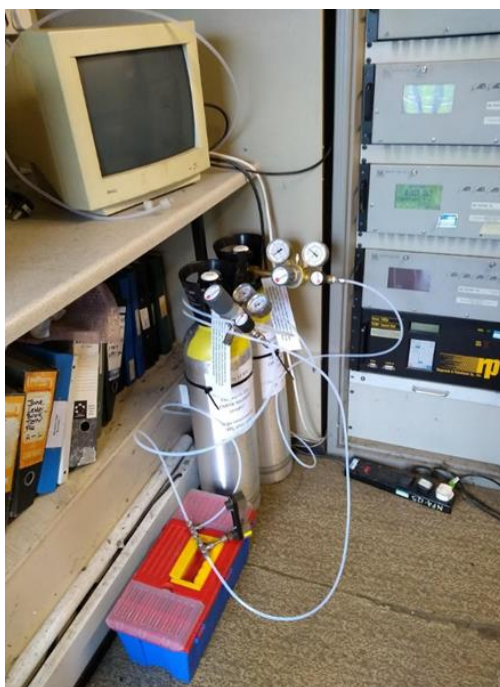


Figure 19: Zero Air and NO<sub>2</sub> Cylinders at ZV1 Sevenoaks Greatness Park (London)

#### Zero- Air Cylinders

Five zero-air cylinders were provided. One cylinder was distributed to each of the five selected LAQN monitoring sites. The site location for each zero-air cylinder is listed in Table 8.

Table 8: Location of zero-air cylinders

Cylinder I.D.	LAQN Monitoring Station
S388R	BX2 - Bexley - Belvedere
S394	ZV1 - Sevenoaks - Greatness Park
S376R	IS2 - Islington - Holloway Road
S348R	IS6 - Islington - Arsenal
S379R	SK6 - Southwark - Elephant & Castle

At each site, the response from the NO<sub>x</sub> instrument was recorded after ten minutes sampling gas from the zero-air cylinder. The zero response from the instrument was also recorded after ten minutes sampling ambient air through the site zero-air scrubber.

Where the difference between the measured NO<sub>x</sub> response from the zero-air cylinder and the measured NO<sub>x</sub> response through the site zero-air scrubber is ≤ 3nmol/mol, the zero-air cylinder NO<sub>x</sub> and NO measurements are used for analysis.

However, where the difference between the measured NO<sub>x</sub> response from the zero-air cylinder and the measured NO<sub>x</sub> response through the zero-air scrubber is > 3nmol/mol, an average of the zero-air cylinder NO<sub>x</sub> and NO measurements and site zero-air scrubber NO<sub>x</sub> and NO measurements are used for analysis.

### NO<sub>2</sub> Cylinders

Five NO<sub>2</sub> cylinders were provided. One cylinder was distributed to each of the five selected LAQN monitoring sites. The site location for each NO<sub>2</sub> cylinder and the instrument type at each site is listed in Table 9.

Table 9: Location of NO<sub>2</sub> cylinders and instrument type.

Cylinder I.D.	LAQN Monitoring Station	Analyser
2791	BX2 - Bexley - Belvedere	Teledyne API M200A/Teledyne API M200E <sup>1</sup>
2902	ZV1 - Sevenoaks - Greatness Park	Monitor Labs ML9841B
2802	IS2 - Islington - Holloway Road	Monitor Labs ML9841B
2907	IS6 - Islington - Arsenal	Monitor Labs ML9841B
2786	SK6 - Southwark - Elephant & Castle	Monitor Labs ML9841B

<sup>1</sup> M200E installed 22/07/2020

At each site the instrument calibration factor (F) was calculated for NO and NO<sub>x</sub> as follows.

$$F = \frac{c}{(V_s - V_z)}$$

Where

c is the certified site NO cylinder amount fraction,

V<sub>s</sub> is the instrument measured span response using the certified site cylinder

V<sub>z</sub> is the instrument measured zero response using the zero-air site scrubber.

The F value is routinely calculated for NO and NO<sub>x</sub> at each Local Site Operator (LSO) calibration. It changes over time as the instrument's response changes, due to normal operational wear and tear or due to specific events such as services and repairs.

At each site the span response (R<sub>s</sub>) is calculated for NO and NO<sub>x</sub> as follows.

$$R_s = R_c - R_z$$

Where R<sub>c</sub> is the NO<sub>2</sub> cylinder measured span response and R<sub>z</sub> is the zero response (zeros for analysis).

The final NO and NO<sub>x</sub> amount fraction is then calculated by applying the instrument calibration factor to the span response as follows.

$$\text{Final amount fraction (nmol/mol)} = F(R_s)$$

The final NO<sub>2</sub> amount fraction is calculated by subtracting the final NO amount fraction from the final NO<sub>x</sub> amount fraction.

$$\text{NO}_2 = \text{NO}_x - \text{NO}$$

### 2.1.3.2 Results

#### 2.1.3.2.1 Zero response

Zero response measurements from the NPL zero-air cylinder, the site zero-air scrubber and zero response measurements for analysis – including averaged values, where applicable – are displayed for each site in Tables 10-14.

Table 10: BX2 - Instrument measured zero response (nmol/mol) and zeros for analysis.

Date	NPL Zero-Air Cylinder		Site Zero-Air Scrubber		Zeros for Analysis	
	NO <sub>x</sub>	NO	NO <sub>x</sub>	NO	NO <sub>x</sub>	NO
26/02/2020	0.6	0.2	-0.2	-0.6	0.6	0.2
24/03/2020	6.7	2.8	2.6	1.8	<b>*4.7</b>	<b>*2.3</b>
23/04/2020	10.8	2.7	3.3	2.6	<b>*7.1</b>	<b>*2.7</b>
22/05/2020	5.4	2.7	1.9	2.5	<b>*3.7</b>	<b>*2.6</b>
17/06/2020	6.7	2.5	1.7	2.5	<b>*4.2</b>	<b>*2.5</b>
03/08/2020	1.7	0.0	-0.9	0.2	1.7	0.0

*\*Averaged zeros*

At BX2, four measurements were also recorded after 5 minutes sampling zero-air gas from the zero-air cylinder. For three of the measurements there was no significant difference between the zero response after 5 minutes and after 10 minutes. On the fourth occasion only the 5 minute zero was measured and this was also used as the 10 minute measurement.

Table 11: ZV1 - Instrument measured zero response (nmol/mol) and zeros for analysis.

Date	NPL Zero-Air Cylinder		Site Zero-Air Scrubber		Zeros for Analysis	
	NO <sub>x</sub>	NO	NO <sub>x</sub>	NO	NO <sub>x</sub>	NO
04/03/2020	5.0	2.0	3.0	0.0	5.0	2.0
13/03/2020	5.0	3.0			5.0	3.0
01/04/2020	9.0	1.0	3.0	1.0	<b>*6.0</b>	<b>*1.0</b>
28/05/2020	12.0	2.0	1.0	0.0	<b>*6.5</b>	<b>*1.0</b>
25/06/2020	11.0	2.0	0.0	-1.0	<b>*5.5</b>	<b>*0.5</b>
20/07/2020	17.0	2.7	-1.0	0.0	<b>*8.0</b>	<b>*1.4</b>
04/08/2020	10.7	1.0	-2.0	-1.0	<b>*4.4</b>	<b>*0.0</b>
21/08/2020	15.7	2.7	0.0	0.0	<b>*7.9</b>	<b>*1.4</b>
02/09/2020	7.0	1.0	0.0	0.0	<b>*3.5</b>	<b>*0.5</b>

*\*Averaged zeros*

At ZV1, one measurement was also recorded after 5 minutes sampling zero-air gas from the zero-air cylinder. No significant difference was observed between the zero response after 5 minutes and after 10 minutes. On one date 13/03/2020 a corresponding measurement from the zero-air scrubber was not recorded.

Table 12: IS2 - Instrument measured zero response (nmol/mol) and zeros for analysis.

Date	NPL Zero-Air Cylinder		Site Zero-Air Scrubber		Zeros for Analysis	
	NO <sub>x</sub>	NO	NO <sub>x</sub>	NO	NO <sub>x</sub>	NO
20/02/2020	3.0	1.0	0.0	-2.0	3.0	1.0
05/03/2020	3.0	3.0	1.0	0.0	3.0	3.0
16/03/2020	1.0	0.0	2.0	0.0	1.0	0.0
18/05/2020	4.3	-1.0	-2.0	-3.0	<b>*1.2</b>	<b>*-2.0</b>
12/06/2020	5.7	1.0	0.0	0.0	<b>*2.9</b>	<b>*0.5</b>
22/06/2020	3.7	1.3	1.0	1.0	3.7	1.3
06/07/2020	4.0	1.0	-2.0	-2.0	<b>*1.0</b>	<b>*-0.5</b>
20/07/2020	4.7	2.3	-1.3	-1.7	<b>*1.7</b>	<b>*0.3</b>
04/08/2020	2.3	0.7	-1.3	-1.0	<b>*0.5</b>	<b>*-0.2</b>

*\*Averaged zeros*

Table 13: IS6 - Instrument measured zero response (nmol/mol) and zeros for analysis.

Date	NPL Zero-Air Cylinder		Site Zero-Air Scrubber		Zeros for Analysis	
	NO <sub>x</sub>	NO	NO <sub>x</sub>	NO	NO <sub>x</sub>	NO
20/02/2020	5.0	2.0	1.0	1.0	<b>*3.0</b>	<b>*1.5</b>
05/03/2020	3.0	1.0	0.0	-1.0	3.0	1.0
16/03/2020	3.0	1.0	0.0	0.0	3.0	1.0
12/05/2020	6.0	1.0	3.0	0.0	6.0	1.0
12/06/2020	7.0	2.0	1.0	0.0	<b>*4.0</b>	<b>*1.0</b>
22/06/2020	6.0	1.3	2.0	0.0	<b>*4.0</b>	<b>*0.7</b>
20/07/2020	6.0	1.0	0.0	0.0	<b>*3.0</b>	<b>*0.5</b>
04/08/2020	6.0	2.0	1.3	0.7	<b>*3.7</b>	<b>*1.4</b>
20/08/2020	8.0	2.0	1.0	-1.0	<b>*4.5</b>	<b>*0.5</b>

*\*Averaged zeros*

Table 14. SK6: Instrument measured zero response (nmol/mol) and zeros for analysis.

Date	NPL Zero-Air Cylinder		Site Zero-Air Scrubber		Zeros for Analysis	
	NO <sub>x</sub>	NO	NO <sub>x</sub>	NO	NO <sub>x</sub>	NO
25/02/2020	1.0	0.0	0.0	-1.0	1.0	0.0
09/03/2020	2.0	1.0	0.0	-1.0	2.0	1.0
25/03/2020	5.0	2.0	1.0	0.0	<b>*3.0</b>	<b>*1.0</b>
28/04/2020	2.0	0.0	1.0	0.0	2.0	0.0
22/05/2020	4.0	1.0	0.0	1.0	<b>*2.0</b>	<b>*1.0</b>
16/06/2020	4.0	1.0	1.0	1.0	4.0	1.0
14/07/2020	3.0	1.0	0.0	1.0	3.0	1.0
11/08/2020	6.0	0.0	1.0	0.0	<b>*3.5</b>	<b>*0.0</b>

*\*Averaged zeros*

### 2.1.3.2.2 NO<sub>2</sub> cylinder response

For these tests, each site instrument's span response to NO<sub>x</sub> and NO was recorded after 5, 10 and 12 minutes sampling gas from the test NPL NO<sub>2</sub> cylinder. Results for each site are displayed in Tables 15-29 and Figures 20-24.

#### Site BX2

Table 15: BX2 NO<sub>2</sub> cylinder 5-min Span Response (R<sub>s</sub>), Instrument Calibration Factor (F) and Final NO, NO<sub>x</sub> and NO<sub>2</sub> Amount Fraction (nmol/mol).

Date	Span Response (R <sub>s</sub> )		Instrument Calibration Factor (F)		Final Amount Fraction (nmol/mol)		
	NO <sub>x</sub>	NO	NO <sub>x</sub>	NO	NO <sub>x</sub>	NO	NO <sub>2</sub>
26/02/2020	543.2	61.1	0.924	0.912	501.9	55.7	446.2
24/03/2020	604.4	45.6	0.953	0.935	576.0	42.6	533.4
23/04/2020	517.9	48.6	1.096	1.079	567.6	52.4	515.2
22/05/2020	528.0	53.1	1.104	1.082	582.9	57.5	525.5
17/06/2020	523.5	53.3	1.105	1.080	578.5	57.6	520.9
03/08/2020	549.5	51.0	1.064	1.047	584.7	53.4	531.3

Table 16: BX2 NO<sub>2</sub> cylinder 10-min Span Response (R<sub>s</sub>), Instrument Calibration Factor (F) and Final NO, NO<sub>x</sub> and NO<sub>2</sub> Amount Fraction (nmol/mol).

Date	Span Response (R <sub>s</sub> )		Instrument Calibration Factor (F)		Final Amount Fraction (nmol/mol)		
	NO <sub>x</sub>	NO	NO <sub>x</sub>	NO	NO <sub>x</sub>	NO	NO <sub>2</sub>
26/02/2020	593.1	67.7	0.924	0.912	548.0	61.7	486.3
24/03/2020	620.1	47.0	0.953	0.935	591.0	43.9	547.0
23/04/2020	572.3	47.1	1.096	1.079	627.2	50.8	576.4
22/05/2020	586.4	49.9	1.104	1.082	647.4	54.0	593.4
17/06/2020	576.6	48.9	1.105	1.080	637.1	52.8	584.3
03/08/2020	614.5	42.5	1.064	1.047	653.8	44.5	609.3

Table 17: BX2 NO<sub>2</sub> cylinder 12-min Span Response (R<sub>s</sub>), Instrument Calibration Factor (F) and Final NO, NO<sub>x</sub> and NO<sub>2</sub> Amount Fraction (nmol/mol).

Date	Span Response (R <sub>s</sub> )		Instrument Calibration Factor (F)		Final Amount Fraction (nmol/mol)		
	NO <sub>x</sub>	NO	NO <sub>x</sub>	NO	NO <sub>x</sub>	NO	NO <sub>2</sub>
26/02/2020	605.3	69.3	0.924	0.912	559.3	63.2	496.1
24/03/2020	671.5	46.8	0.953	0.935	639.9	43.8	596.2
23/04/2020	581.4	46.2	1.096	1.079	637.2	49.8	587.4
22/05/2020	597.7	48.8	1.104	1.082	659.9	52.8	607.1
17/06/2020	586.8	47.4	1.105	1.080	648.4	51.2	597.2
03/08/2020	624.0	42.0	1.064	1.047	663.9	44.0	620.0

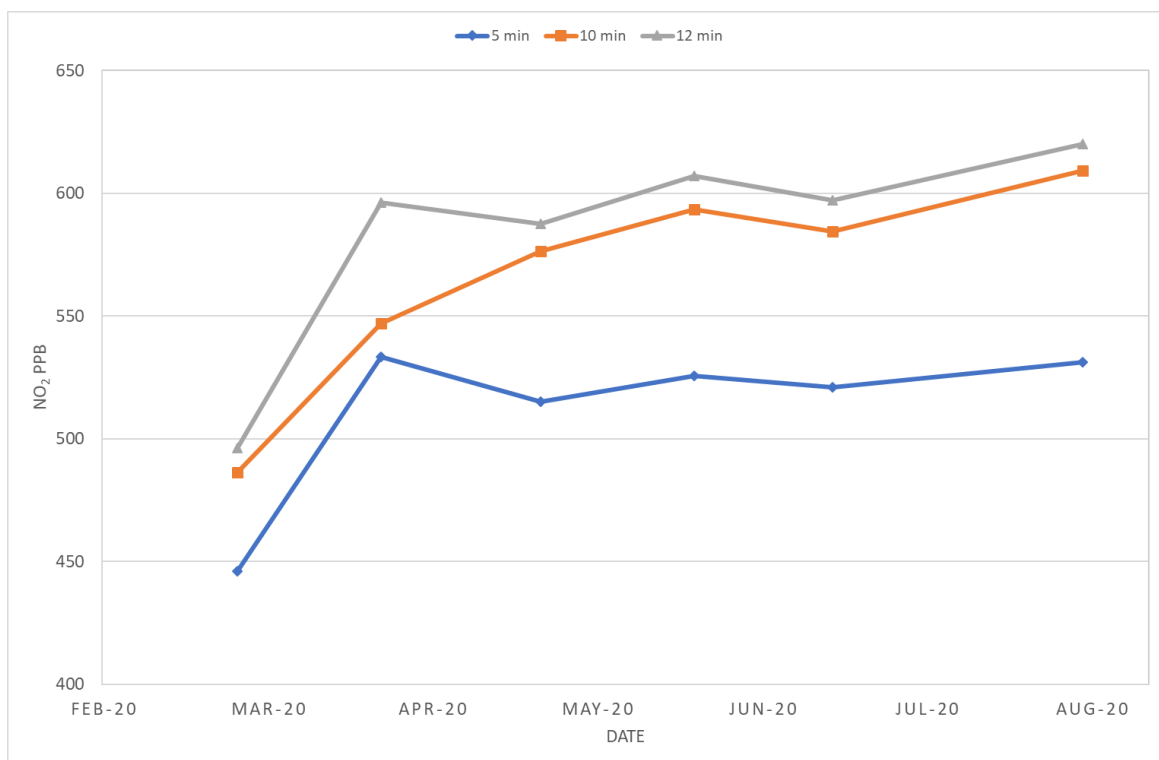


Figure 20: BX2 NO<sub>2</sub> cylinder – NO<sub>2</sub> final calculated amount fractions (in nmol/mol) for 5, 10 and 12-minute spans.



Site ZV1

Table 18: ZV1 NO2 cylinder 5-min Span Response (Rs), Instrument Calibration Factor (F) and Final NO, NOx and NO2 Amount Fraction (nmol/mol).

Date	Span Response (Rs)		Instrument Calibration Factor (F)		Final Amount Fraction (nmol/mol)		
	NO <sub>x</sub>	NO	NO <sub>x</sub>	NO	NO <sub>x</sub>	NO	NO <sub>2</sub>
04/03/2020	538.0	20.3	1.383	1.536	744.1	31.2	712.9
13/03/2020	529.0	13.0	1.447	1.597	765.2	20.8	744.4
01/04/2020	773.3	24.7	1.023	1.102	791.1	27.2	763.9
09/04/2020	776.7	27.0	1.070	1.091	831.1	29.5	801.6
28/05/2020	761.8	18.0	1.138	1.190	866.9	21.4	845.5
25/06/2020	685.8	15.8	1.240	1.318	850.4	20.8	829.6
20/07/2020	747.7	21.9	1.144	1.153	855.4	25.3	830.1
04/08/2020	742.9	19.0	1.156	1.203	858.8	22.9	835.9
21/08/2020	715.1	17.6	1.197	1.244	856.0	21.9	834.1
02/09/2020	731.2	18.5	1.178	1.237	861.4	22.9	838.5

Table 19: ZV1 NO2 cylinder 10-min Span Response (Rs), Instrument Calibration Factor (F) and Final NO, NOx and NO2 Amount Fraction (nmol/mol).

Date	Span Response (Rs)		Instrument Calibration Factor (F)		Final Amount Fraction (nmol/mol)		
	NO <sub>x</sub>	NO	NO <sub>x</sub>	NO	NO <sub>x</sub>	NO	NO <sub>2</sub>
04/03/2020	562.3	25.0	1.383	1.536	777.7	38.4	739.3
13/03/2020	563.0	18.0	1.447	1.597	814.4	28.7	785.6
01/04/2020	779.3	31.7	1.023	1.102	797.2	34.9	762.3
09/04/2020	815.3	31.0	1.070	1.091	872.4	33.8	838.6
28/05/2020	780.5	20.7	1.138	1.190	888.2	24.6	863.6
25/06/2020	702.8	17.5	1.240	1.318	871.5	23.1	848.4
20/07/2020	765.7	26.3	1.144	1.153	876.0	30.3	845.6
04/08/2020	759.9	21.0	1.156	1.203	878.4	25.3	853.2
21/08/2020	733.1	20.6	1.197	1.244	877.5	25.6	851.9
02/09/2020	741.2	21.8	1.178	1.237	873.1	27.0	846.2

Table 20: ZV1 NO<sub>2</sub> cylinder 12-min Span Response (R<sub>s</sub>), Instrument Calibration Factor (F) and Final NO, NO<sub>x</sub> and NO<sub>2</sub> Amount Fraction (nmol/mol).

Date	Span Response (R <sub>s</sub> )		Instrument Calibration Factor (F)		Final Amount Fraction (nmol/mol)		
	NO <sub>x</sub>	NO	NO <sub>x</sub>	NO	NO <sub>x</sub>	NO	NO <sub>2</sub>
13/02/2020	547.0	28.0	1.375	1.521	752.1	42.6	709.5
04/03/2020	578.3	25.0	1.383	1.536	799.8	38.4	761.4
13/03/2020	571.0	18.0	1.447	1.597	826.0	28.7	797.2
01/04/2020	794.0	32.3	1.023	1.102	812.3	35.6	776.7
09/04/2020	827.7	33.0	1.070	1.091	885.6	36.0	849.6
28/05/2020	786.8	21.0	1.138	1.190	895.4	25.0	870.4
25/06/2020	712.2	18.8	1.240	1.318	883.1	24.8	858.3
20/07/2020	772.3	28.6	1.144	1.153	883.5	33.0	850.5
04/08/2020	768.3	23.7	1.156	1.203	888.2	28.5	859.6
21/08/2020	738.1	21.6	1.197	1.244	883.5	26.9	856.6
02/09/2020	745.5	22.5	1.178	1.237	878.2	27.8	850.4

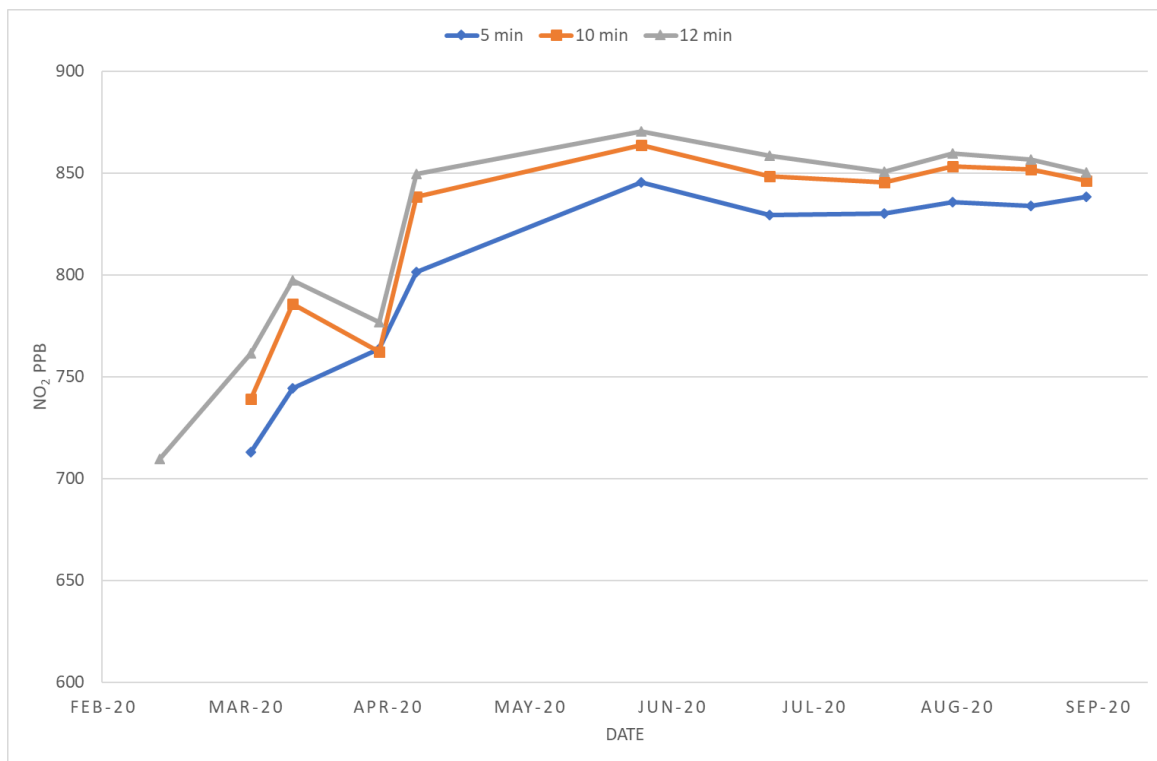


Figure 21: ZV1 NO<sub>2</sub> cylinder – NO<sub>2</sub> final calculated amount fractions (nmol/mol) for 5, 10 and 12-minute spans.

Site IS2

Table 21: IS2 NO<sub>2</sub> cylinder 5-min Span Response (R<sub>s</sub>), Instrument Calibration Factor (F) and Final NO, NO<sub>x</sub> and NO<sub>2</sub> Amount Fraction (nmol/mol).

Date	Span Response (R <sub>s</sub> )		Instrument Calibration Factor (F)		Final Amount Fraction (nmol/mol)		
	NO <sub>x</sub>	NO	NO <sub>x</sub>	NO	NO <sub>x</sub>	NO	NO <sub>2</sub>
20/02/2020	690.0	24.0	1.070	1.045	738.3	25.1	713.2
05/03/2020	552.0	22.0	1.306	1.279	720.9	28.1	692.8
16/03/2020	566.0	25.0	1.296	1.271	733.5	31.8	701.8
18/05/2020	592.8	23.0	1.244	1.232	737.4	28.3	709.1
12/06/2020	559.1	20.5	1.240	1.232	693.3	25.3	668.0
22/06/2020	645.3	15.7	1.161	1.138	749.2	17.9	731.3
06/07/2020	662.0	19.5	1.178	1.167	779.8	22.8	757.1
20/07/2020	698.3	22.7	1.089	1.078	760.4	24.5	736.0
04/08/2020	704.5	19.2	1.079	1.065	760.2	20.4	739.8

Table 22: IS2 NO<sub>2</sub> cylinder 10-min Span Response (R<sub>s</sub>), Instrument Calibration Factor (F) and Final NO, NO<sub>x</sub> and NO<sub>2</sub> Amount Fraction (nmol/mol).

Date	Span Response (R <sub>s</sub> )		Instrument Calibration Factor (F)		Final Amount Fraction (nmol/mol)		
	NO <sub>x</sub>	NO	NO <sub>x</sub>	NO	NO <sub>x</sub>	NO	NO <sub>2</sub>
20/02/2020	732.0	24.0	1.070	1.045	783.2	25.1	758.2
05/03/2020	-	-	1.306	1.279	-	-	-
16/03/2020	611.0	22.0	1.296	1.271	791.9	28.0	763.9
18/05/2020	624.8	23.0	1.244	1.232	777.3	28.3	748.9
12/06/2020	598.1	22.5	1.240	1.232	741.6	27.7	713.9
22/06/2020	666.3	20.7	1.161	1.138	773.6	23.6	750.0
06/07/2020	656.0	18.5	1.178	1.167	772.8	21.6	751.2
20/07/2020	711.3	20.7	1.089	1.078	774.6	22.3	752.3
04/08/2020	728.5	23.2	1.079	1.065	786.1	24.7	761.4

Table 23: IS2 NO<sub>2</sub> cylinder 12-min Span Response (R<sub>s</sub>), Instrument Calibration Factor (F) and Final NO, NO<sub>x</sub> and NO<sub>2</sub> Amount Fraction (nmol/mol).

Date	Span Response (R <sub>s</sub> )		Instrument Calibration Factor (F)		Final Amount Fraction (nmol/mol)		
	NO <sub>x</sub>	NO	NO <sub>x</sub>	NO	NO <sub>x</sub>	NO	NO <sub>2</sub>
20/02/2020	742.0	25.0	1.070	1.045	793.9	26.1	767.8
05/03/2020	599.0	19.0	1.306	1.279	782.3	24.3	758.0
16/03/2020	621.0	23.0	1.296	1.271	804.8	29.2	775.6
18/05/2020	624.8	22.0	1.244	1.232	777.3	27.1	750.1
12/06/2020	614.1	21.5	1.240	1.232	761.5	26.5	735.0
22/06/2020	675.3	19.7	1.161	1.138	784.0	22.4	761.6
06/07/2020	660.0	17.5	1.178	1.167	777.5	20.4	757.1
20/07/2020	716.3	19.7	1.089	1.078	780.1	21.2	758.8
04/08/2020	732.5	22.2	1.079	1.065	790.4	23.6	766.8

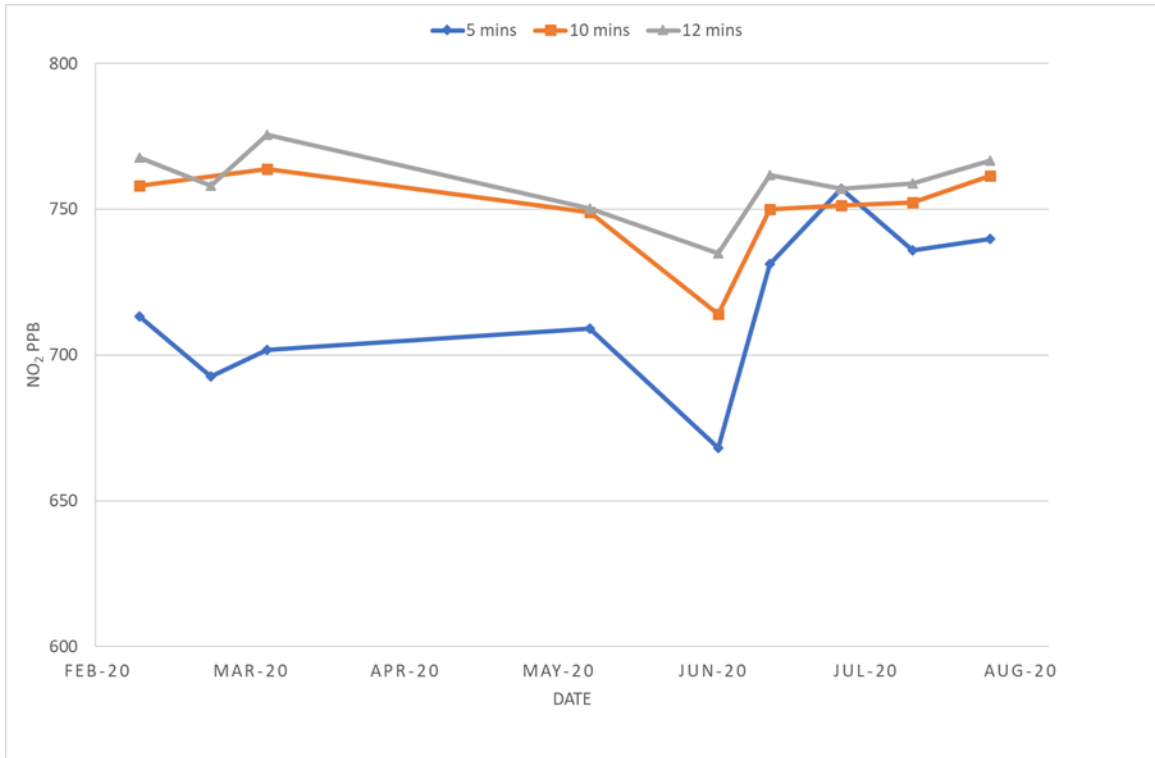


Figure 22: IS2 NO<sub>2</sub> cylinder – NO<sub>2</sub> final calculated amount fractions (nmol/mol) for 5, 10 and 12-minute spans.

### Site IS6

Table 24: IS6 NO<sub>2</sub> cylinder 5-min Span Response (R<sub>s</sub>), Instrument Calibration Factor (F) and Final NO, NO<sub>x</sub> and NO<sub>2</sub> Amount Fraction (nmol/mol).

Date	Span Response (R <sub>s</sub> )		Instrument Calibration Factor (F)		Final Amount Fraction (nmol/mol)		
	NO <sub>x</sub>	NO	NO <sub>x</sub>	NO	NO <sub>x</sub>	NO	NO <sub>2</sub>
20/02/2020	608.0	19.5	1.186	1.191	720.8	23.2	697.6
05/03/2020	723.0	26.0	1.007	1.023	728.1	26.6	701.5
16/03/2020	753.0	23.0	1.015	1.052	764.3	24.2	740.1
12/05/2020	681.0	21.0	1.093	1.140	744.3	23.9	720.4
12/06/2020	643.0	20.0	1.131	1.140	727.2	22.8	704.4
22/06/2020	658.0	20.4	1.134	1.152	746.2	23.4	722.7
20/07/2020	641.0	18.5	1.158	1.155	742.3	21.4	720.9
04/08/2020	630.4	20.7	1.170	1.168	737.5	24.1	713.4
20/08/2020	585.5	22.5	1.238	1.185	724.8	26.7	698.2

Table 25: IS6 NO<sub>2</sub> cylinder 10-min Span Response (R<sub>s</sub>), Instrument Calibration Factor (F) and Final NO, NO<sub>x</sub> and NO<sub>2</sub> Amount Fraction (nmol/mol).

Date	Span Response (R <sub>s</sub> )		Instrument Calibration Factor (F)		Final Amount Fraction (nmol/mol)		
	NO <sub>x</sub>	NO	NO <sub>x</sub>	NO	NO <sub>x</sub>	NO	NO <sub>2</sub>
20/02/2020	653.0	21.5	1.186	1.191	774.1	25.6	748.5
05/03/2020	757.0	26.0	1.007	1.023	762.3	26.6	735.7
16/03/2020	764.0	23.0	1.015	1.052	775.5	24.2	751.3
12/05/2020	688.0	21.0	1.093	1.140	752.0	23.9	728.0
12/06/2020	672.0	20.0	1.131	1.140	760.0	22.8	737.2
22/06/2020	671.0	20.4	1.134	1.152	760.9	23.4	737.5
20/07/2020	656.0	20.5	1.158	1.155	759.6	23.7	736.0
04/08/2020	646.4	17.7	1.170	1.168	756.2	20.6	735.6
20/08/2020	602.5	21.5	1.238	1.185	745.9	25.5	720.4

Table 26: IS6 NO<sub>2</sub> cylinder 12-min Span Response (R<sub>s</sub>), Instrument Calibration Factor (F) and Final NO, NO<sub>x</sub> and NO<sub>2</sub> Amount Fraction (nmol/mol).

Date	Span Response (R <sub>s</sub> )		Instrument Calibration Factor (F)		Final Amount Fraction (nmol/mol)		
	NO <sub>x</sub>	NO	NO <sub>x</sub>	NO	NO <sub>x</sub>	NO	NO <sub>2</sub>
20/02/2020	669.0	21.5	1.186	1.191	793.1	25.6	767.5
05/03/2020	765.0	29.0	1.007	1.023	770.4	34.5	735.8
16/03/2020	773.0	23.0	1.015	1.052	784.6	27.4	757.2
12/05/2020	695.0	20.0	1.093	1.140	759.6	23.8	735.8
12/06/2020	675.0	20.0	1.131	1.140	763.4	23.8	739.6
22/06/2020	676.0	20.4	1.134	1.152	766.6	24.2	742.4
20/07/2020	661.0	21.5	1.158	1.155	765.4	25.6	739.8
04/08/2020	653.4	18.7	1.170	1.168	764.4	22.2	742.2
20/08/2020	605.5	21.5	1.238	1.185	749.6	25.6	724.0

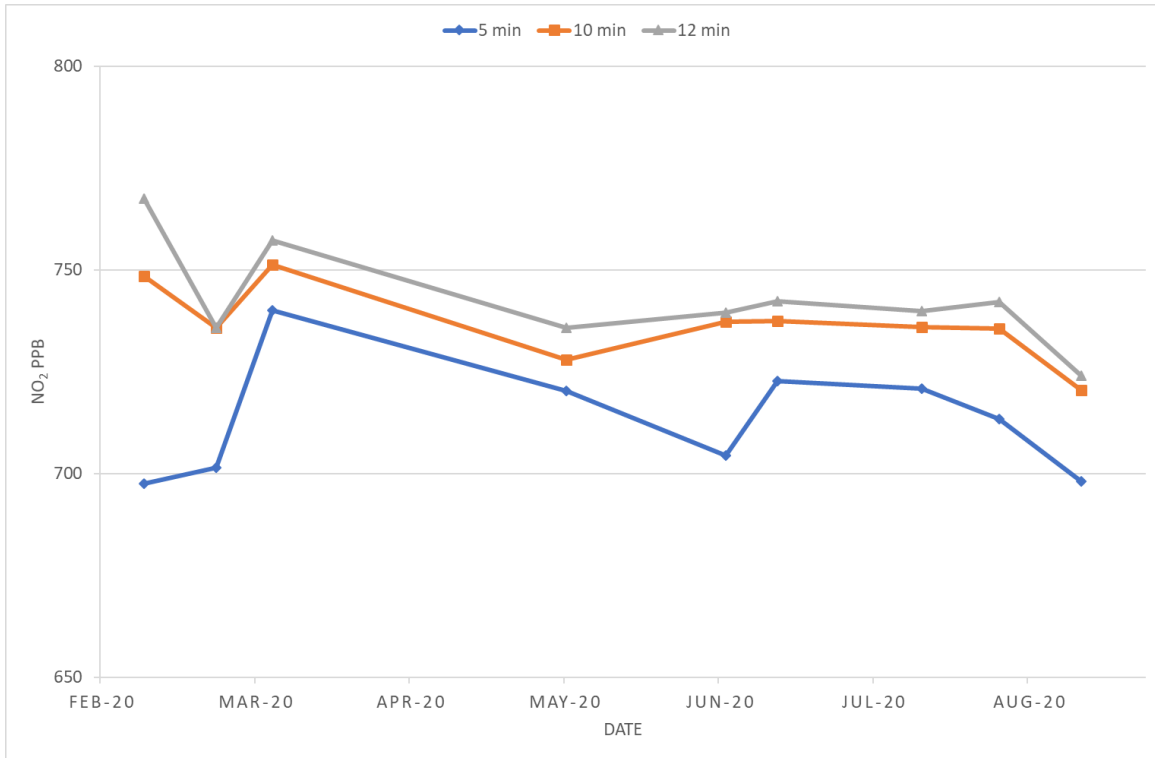


Figure 23: IS6 NO<sub>2</sub> cylinder – NO<sub>2</sub> final calculated amount fractions (nmol/mol) for 5, 10 and 12-minute spans.

### Site SK6

Table 27: SK6 NO<sub>2</sub> cylinder 5-min Span Response (R<sub>s</sub>), Instrument Calibration Factor (F) and Final NO, NO<sub>x</sub> and NO<sub>2</sub> Amount Fraction (nmol/mol).

Date	Span Response (R <sub>s</sub> )		Instrument Calibration Factor (F)		Final Amount Fraction (nmol/mol)		
	NO <sub>x</sub>	NO	NO <sub>x</sub>	NO	NO <sub>x</sub>	NO	NO <sub>2</sub>
25/02/2020	660.0	22.0	1.159	1.206	764.9	26.5	738.4
09/03/2020	767.0	27.0	1.029	1.053	789.2	28.4	760.8
25/03/2020	725.0	26.0	1.103	1.121	799.7	29.1	770.5
28/04/2020	593.0	23.0	1.254	1.297	743.6	29.8	713.8
22/05/2020	586.0	24.0	1.294	1.339	758.3	32.1	726.1
16/06/2020	570.0	21.0	1.329	1.368	757.5	28.7	728.8
14/07/2020	555.0	19.0	1.361	1.393	755.4	26.5	728.9
11/08/2020	548.5	20.0	1.421	1.395	779.4	27.9	751.5

Table 28: SK6 NO<sub>2</sub> cylinder 10-min Span Response (R<sub>s</sub>), Instrument Calibration Factor (F) and Final NO, NO<sub>x</sub> and NO<sub>2</sub> Amount Fraction (nmol/mol).

Date	Span Response (R <sub>s</sub> )		Instrument Calibration Factor (F)		Final Amount Fraction (nmol/mol)		
	NO <sub>x</sub>	NO	NO <sub>x</sub>	NO	NO <sub>x</sub>	NO	NO <sub>2</sub>
25/02/2020	709.0	29.0	1.159	1.206	821.7	35.0	786.8
09/03/2020	783.0	27.0	1.029	1.053	805.7	28.4	777.3
25/03/2020	737.0	26.0	1.103	1.121	812.9	29.1	783.8
28/04/2020	632.0	23.0	1.254	1.297	792.5	29.8	762.7
22/05/2020	598.0	24.0	1.294	1.339	773.8	32.1	741.7
16/06/2020	578.0	21.0	1.329	1.368	768.2	28.7	739.4
14/07/2020	564.0	21.0	1.361	1.393	767.6	29.3	738.4
11/08/2020	550.5	20.0	1.421	1.395	782.3	27.9	754.4

Table 29: SK6 NO<sub>2</sub> cylinder 12-min Span Response (R<sub>s</sub>), Instrument Calibration Factor (F) and Final NO, NO<sub>x</sub> and NO<sub>2</sub> Amount Fraction (nmol/mol).

Date	Span Response (R <sub>s</sub> )		Instrument Calibration Factor (F)		Final Amount Fraction (nmol/mol)		
	NO <sub>x</sub>	NO	NO <sub>x</sub>	NO	NO <sub>x</sub>	NO	NO <sub>2</sub>
25/02/2020	711.0	26.0	1.159	1.206	824.0	31.4	792.7
09/03/2020	789.0	26.0	1.029	1.053	811.9	27.4	784.5
25/03/2020	739.0	26.0	1.103	1.121	815.1	29.1	786.0
28/04/2020	634.0	22.0	1.254	1.297	795.0	28.5	766.5
22/05/2020	603.0	24.0	1.294	1.339	780.3	32.1	748.1
16/06/2020	581.0	22.0	1.329	1.368	772.1	30.1	742.1
14/07/2020	570.0	21.0	1.361	1.393	775.8	29.3	746.5
11/08/2020	552.5	21.0	1.421	1.395	785.1	29.3	755.8

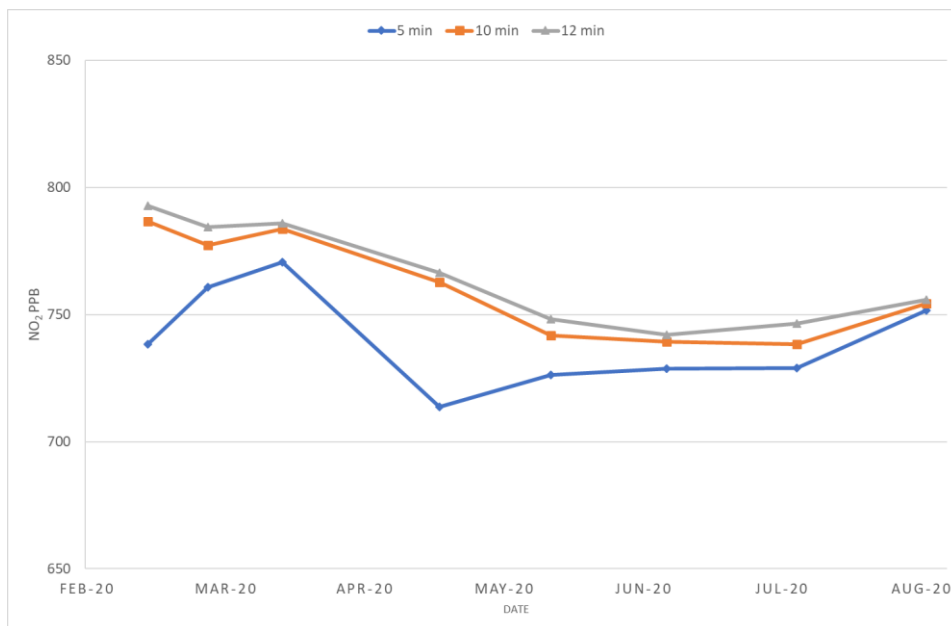


Figure 24: SK6 NO<sub>2</sub> cylinder – NO<sub>2</sub> final calculated amount fractions (nmol/mol) for 5, 10 and 12-minute spans.

## NO<sub>2</sub> cylinder drift

Linear regression (ordinary least squares) was used to calculate the rate of change over time for each cylinder. These regressions and rate of change values are shown in Figures 25-26 and Table 30.

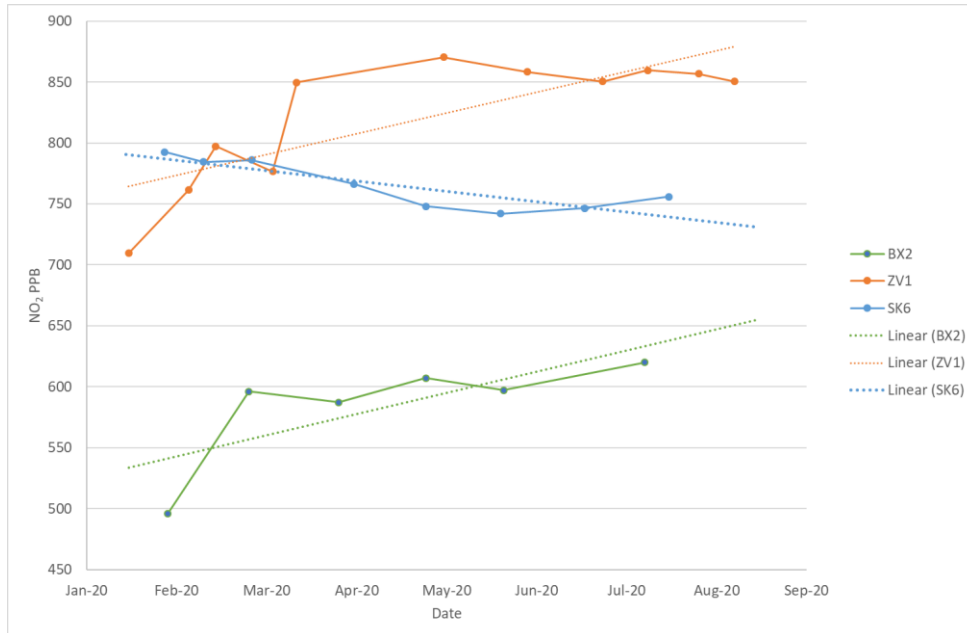


Figure 25: 12 min NO<sub>2</sub> final amount fraction spans and trendlines at sites BX2, ZV1 and SK6

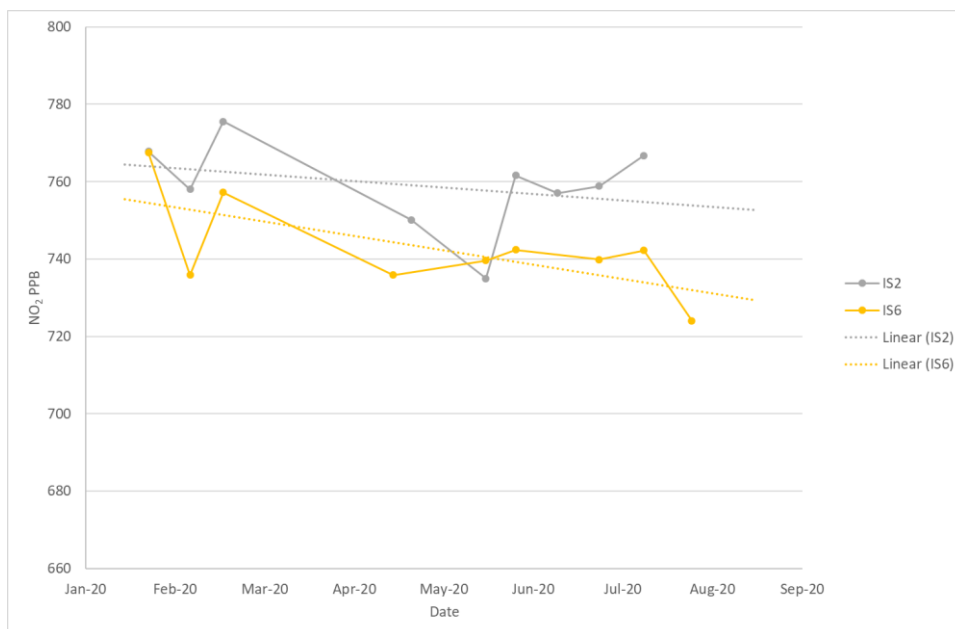


Figure 26: 12 min NO<sub>2</sub> final amount fraction spans and trendlines at sites IS2 and IS6

Table 30: NO<sub>2</sub> Initial and Final Spans (nmol/mol), with calculated change in NO<sub>2</sub> over time and rate of change per day



Site	Initial NO <sub>2</sub> Span		Final NO <sub>2</sub> Span		Δ Initial & Final NO <sub>2</sub> Span		Δ /Day ppb
	Date	ppb	Date	ppb	Days	ppb	
BX2	26/02/2020	496.1	03/08/2020	620.0	159	123.9	0.78
ZV1	13/02/2020	709.5	02/09/2020	850.4	202	140.9	0.70
IS2	20/02/2020	767.8	04/08/2020	766.8	166	-1.0	-0.01
IS6	20/02/2020	767.5	20/08/2020	724.0	182	-43.5	-0.24
SK6	25/02/2020	792.7	11/08/2020	755.8	168	-36.9	-0.22

### 2.1.3.3 Comparison with certified amount fractions

Before NO<sub>2</sub> cylinders were distributed to the monitoring sites their NO<sub>2</sub> amount fractions were measured by NPL. It was planned to measure amount fractions again at the end of the project when cylinders had been removed from the sites, however Covid restrictions meant this was not possible. Results from the initial NPL measurement before deployment as well as the initial and final NO<sub>2</sub> measurements as determined by calibrations at sites during the project are presented in Table 31. This provides a snapshot of the difference between certified cylinder NO<sub>2</sub> values and those determined at sites during the project.

Table 31: NPL NO<sub>2</sub> certified amount fractions before deployment and on-site (ERG) NO<sub>2</sub> measured at initial and final calibration.

Cylinder I.D.	LAQN Monitoring Station	Initial NPL	Initial ERG	Final ERG
		Certified NO <sub>2</sub> (ppb)	12 min Cal NO <sub>2</sub> (ppb)	12 min Cal NO <sub>2</sub> (ppb)
npl 2791	BX2 - Bexley - Belvedere	988	496	620
npl 2902	ZV1 - Sevenoaks - Greatness Park	1050	710	850
npl 2802	IS2 - Islington - Holloway Road	1000	768	767
npl 2907	IS6 - Islington - Arsenal	985	768	724
npl 2786	SK6 - Southwark - Elephant & Castle	987	793	756

### 2.1.3.4 Discussion

For all five sites, the in-field response to NO<sub>2</sub> increased with sample time. This can be seen from plots of the 5-, 10- and 12-minute spans. All five sites show a clear distinction between each time interval, with a large difference generally between each 5-minute and 10-minute span, and a smaller but clear difference between 10-minute and 12-minute span responses. The plots indicate that even after 12 minutes the instrument response had likely not stabilized. During routine calibrations with introduced certified NO span gas, typically we would see an instrument response to NO gas stabilizing 5 minutes after the span commences with no significant difference between 5-, 10- and 12-minute spans. To minimize the loss of ambient data, longer tests were not possible to determine if the instrument response had stabilized after 12 minutes.

Over the duration of these tests, two cylinders showed increases over time. Three cylinders showed relative stability. While it would be expected that cylinder wall interactions or reactions of NO<sub>2</sub> with water vapor may affect NO<sub>2</sub> in the cylinder, leading to decreased amount fractions over time, it is harder to account for increased apparent amount fractions. Increases might have been due to conditioning of the regulator or sample lines over time. It should also be noted that both sites BX2

and ZV1, which recorded increases, had a significant response change, after the instruments were serviced in March 2020. In addition, the initial NO<sub>2</sub> calibration span response at ZV1 at installation was significantly lower than all the other calibrations. Removal of these calibrations would have resulted in the response from NO<sub>2</sub> cylinders at these two sites being relatively stable, with slight increase, over the course of the project, as observed at the other three sites.

Certified NO<sub>2</sub> values measured before cylinder deployment were provided for each cylinder. For all cylinders the NO<sub>2</sub> amount fractions measured onsite were lower than the certified values. At BX2 the 12-minute span NO<sub>2</sub> amount fractions measured over the course of the project ranged from 37 % to 50 % lower than the certified value. ZV1 measured 12-minute spans ranged from 17 % to 32 % lower. IS2 12-minute spans ranged from 22 % to 26 % lower. Similarly, IS6 12-minute spans ranged from 22 % to 26 % lower. SK6 12-min spans ranged from 20 % to 25 % lower than initial certified NO<sub>2</sub> values. A comparison with final certified NO<sub>2</sub> values after cylinders were collected from site was not possible due to Covid restrictions, which affect the measurement procedure at NPL.

The high amount fraction of NO<sub>2</sub> in the test cylinders should also be considered. Typically, NO cylinders used for calibrations at ambient sites typically contain around 450 nmol/mol NO. The NO<sub>2</sub> amount fractions in the test cylinders ranged from 985 nmol/mol to 1050 nmol/mol, greater than twice the calibration value for the NO cylinder being used to determine the test cylinder NO<sub>2</sub> amount fraction. For future analysis it would be useful to test NO<sub>2</sub> cylinders with NO<sub>2</sub> amount fractions within the range of the site NO certified cylinder amount fraction.

#### 2.1.3.5 Summary

The stability of the cylinders used in this section (2.1.3) was tested in field deployments at chemiluminescent measurement sites in London.

When used in the field:

- NO<sub>2</sub> amount fractions measured by field instruments were considerably less than that certified amount fraction measured prior to the field test. This difference ranged between 17 and 50 % of the certified amount fraction.
- The field instruments took more than 12 minutes to stabilise when challenged with the test gas.
- Over the duration of the project, two cylinders showed increases over time. Three cylinders showed relative stability. Rates of change were between +0.78 and -0.22 nmol/mol day<sup>-1</sup>.

Due to COVID restrictions, it was not possible to re-test the cylinder amount fraction in the laboratory at the end of the project.

Results from this project suggest that calibration with the traceable and certified NO<sub>2</sub> cylinders would not be suitable for traceable calibrations of instrumentation in the field.

The reasons for this are unclear. The cylinders may have experienced a one-off rapid change in the NO<sub>2</sub> amount fractions soon after certification or during field installation. It is also possible that NO<sub>2</sub> was lost in the site regulator and pipework, affecting the amount fraction delivered from the certified cylinder to the instrument. The increase in instrument response to NO<sub>2</sub> during each

calibration and (at some locations) over the whole project may have been due to gradual conditioning of the regulator and pipework.

### 2.1.3.6 Note on impacts on COVID restrictions on the project

Cylinders were distributed to air quality monitoring sites during the first half of February 2020. On the 23<sup>rd</sup> March 2020, restrictions on freedom of movement were enforced by the British Government due to Covid. These restrictions – in place for the duration of most of these tests – reduced the overall frequency of planned calibrations to the extent that planned fortnightly calibrations were instead carried out monthly, in most cases.

Another consequence of Covid restrictions was that NPL facilities were not operating as usual to enable retesting of the NO<sub>2</sub> amount fraction in cylinders at the end of the field deployments.

## 2.2 Comparison 2 – A2.3.2 outputs

A2.3.2 involved an assessment of ambient NO<sub>x</sub> data quality using the standard reference method of chemiluminescence detection (CLD) versus cavity attenuated phase shift spectroscopy (CAPS), a direct NO<sub>2</sub> measurement technique. The activity consisted of two field deployments at two London Air Quality Network (LAQN) monitoring sites (see Table 32).

Table 32: List of sites and instruments used in comparison 2

Site	Site type	Number of instruments	Instruments type
Marylebone Road (MR)	urban traffic	3	CAPS (1), CLD (2)
Honor Oak Park (HOP)	urban background	3	CAPS (1), CLD (2)

### 2.2.1 Experimental setup

#### 2.2.1.1 Measurement location

NO<sub>x</sub> measurements were carried out at two sites - London Marylebone Road and London Honor Oak Park.

- Marylebone Road (MR, latitude/longitude: 51.522530, -0.154611) is an urban traffic site located in central London, adjacent to a congested road with 6 lanes of traffic. Valid NO<sub>x</sub> measurements were recorded between July and October 2019.
- Honor Oak Park (HOP, latitude/longitude: 51.522530, -0.154611) is an urban background site located in South East London. The site is situated in a sports ground away from major pollution sources and is considered to be representative of background amount fractions in the urban residential area.

A vast range of pollutants are routinely monitored at each LAQN site. Further information about Marylebone Road can be found in [here](#). More details about the site at Honor Oak Park can be found [here](#).

#### 2.2.1.2 NO<sub>x</sub> measurements

Three analysers were set up at each measurement site (6 analysers operated in total).

NO<sub>2</sub> was measured directly using a Teledyne (model T500U) CAPS analyser. This instrument relies on cavity attenuated phase shift spectroscopy. In brief, the CAPS NO<sub>2</sub> analyser consists of a 430 nm LED and an optically resonant cavity formed by two high reflectivity mirrors. The presence of NO<sub>2</sub> in the cell causes a phase shift in the signal received by a photodetector that is proportional to the NO<sub>2</sub> amount fraction.

Two chemiluminescence analysers were used to measure NO and NO<sub>2</sub>. The T200 NO<sub>x</sub> analyser ('Moly') uses a molybdenum converter and the T200UP ('BLC') contains a photolytic converter.

#### 2.2.1.3 Calibration

Zero checks were carried out using a zero air cylinder supplied by NPL. These were prepared gravimetrically at NPL using high purity nitrogen (BIP+, Air Products) and N6.0 oxygen (BOC). For additional details see section 2.1.3.3.

NO cylinders (450 nmol/mol) supplied by Air Liquide were used as span gas for the NO<sub>x</sub> CLD analysers.

A BTCA 178 air cylinder and a 5 µmol/mol NO cylinder (both supplied by BOC) were connected to an Environics 6100 multigas calibrator, which was used to generate NO<sub>2</sub> by gas phase titration (NO + O<sub>3</sub>). The amount fraction of NO<sub>2</sub> formed was calculated from the reduction in the NO signal upon addition of O<sub>3</sub>. The NO<sub>2</sub> generated was used to calculate the conversion efficiency of the NO<sub>x</sub> chemiluminescence analysers and as a span gas for the CAPS NO<sub>2</sub> analyser.

### 2.2.2 Urban traffic site results – Marylebone Road

#### 2.2.2.1 NO measurements

Compared to the urban background site (see 3.2.3), the NO<sub>x</sub> amount fractions are significantly higher and more ariable at Marylebone Road. This site is an urban traffic site located next to a major road that experiences high volumes of traffic throughout the day.

During the day, high levels of NO mixing ratios (approx. 100 - 200 nmol/mol) are frequently measured at Marylebone Road using the T200 ('Moly') and T200UP ('BLC') NO<sub>x</sub> analysers. Peaks above 200 nmol/mol are also observed. Minimum levels of NO are observed overnight when traffic levels are lower, at amount fractions of approximately 20 nmol/mol. The data were scaled according to the cylinder calibration factors.

Figure 27 shows the hourly average NO amount fractions grouped by day of the week, as well as average NO mixing ratios for each month of the measurement period. The average daytime NO amount fraction throughout the measurement period was 80 nmol/mol, dropping to 10-20 nmol/mol overnight. NO amount fractions were 25-50% lower on the weekends compared to the weekdays.

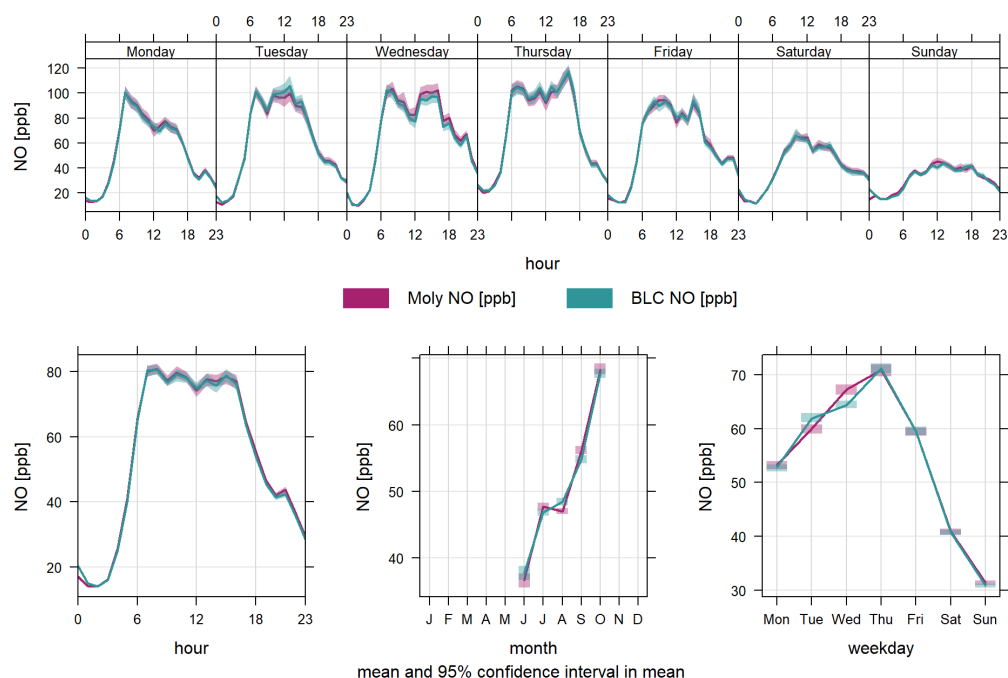


Figure 27: Ambient NO measurements at Marylebone Road (25/06/2019 to 30/10/2019) on a daily, weekly and monthly basis.

The 1-min and hourly correlations in NO measurements recorded by the BLC and Moly analysers are shown in Figure 28 and Figure 19 respectively. Significant differences between the two instruments can be seen in the 1-min data; due to the nature of the site, there is high variation in the NO levels, so the observed amount fraction differences in each 1 minute interval are presumably due to differing flow rates/instrument response times. Strong agreement between the BLC and Moly analysers is observed for the hourly averaged NO data ( $R^2 = 0.99$ ).

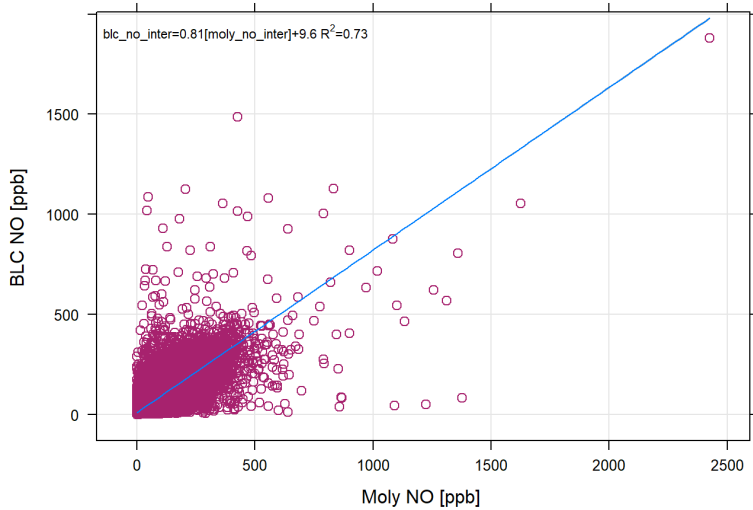


Figure 28: Comparison of NO measured using the BLC and Moly analysers (1 min data).

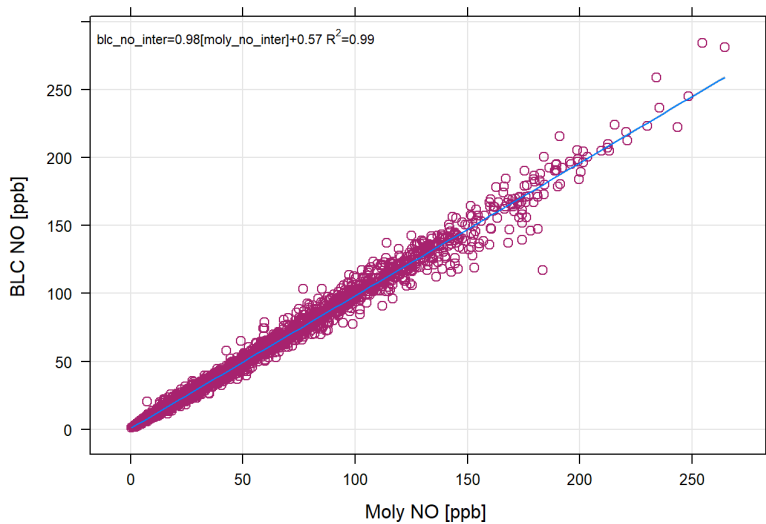


Figure 19: Comparison of NO measured using the BLC and Moly analysers (hourly data)

### 2.2.2.2 NO<sub>2</sub> measurements

NO<sub>2</sub> mixing ratios were measured at Marylebone Road using the Moly, BLC and CAPS analysers. The data were scaled according to the cylinder calibration factors and calculated conversion efficiencies. NO<sub>2</sub> levels at the roadside site remain high throughout the day (100 - 200 nmol/mol). High variation is observed, which is likely due to the primary NO<sub>2</sub> emissions from traffic passing directly past the site. The lowest NO<sub>2</sub> amount fractions (approximately 20 nmol/mol) are recorded overnight.

The observed CAPS NO<sub>2</sub> signal (orange line) looks very different to the Moly and BLC NO<sub>2</sub> signals. The CAPS analyser does not appear to show as much variation in the NO<sub>2</sub> amount fraction and the signal is more compressed than the CLD signals. This effect is not apparent in the hourly time series as it has been averaged out. This is an important observation because it suggests that differences in instrument response / flow rate can significantly alter reported NO<sub>2</sub> amount fractions at busy roadside sites. Further investigation is needed to establish how this can be improved. Figure 30 shows a comparison of the average hourly NO<sub>2</sub> signals recorded by the Moly, BLC and CAPS analyser,

categorised according to day of the week, month, and measurement campaign. Although relatively good agreement is seen overnight when NO<sub>2</sub> levels are lowest, poor agreement is seen during the day when NO<sub>2</sub> levels are high. Interestingly both CLD's show a higher signal than the CAPS NO<sub>2</sub> analyser, and the BLC is higher than the Moly during the day. Further research is needed to establish the true variation in the NO<sub>2</sub> amount fractions at the site and the influence of possible interfering compounds. This would help to optimise the best instrument set up at urban traffic sites.

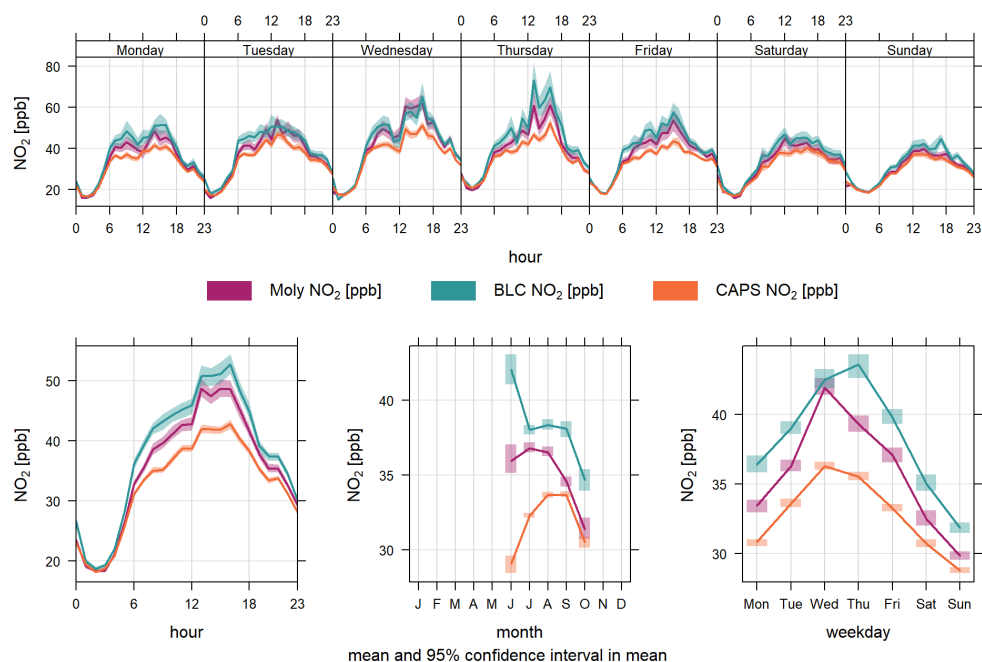


Figure 30: Ambient NO<sub>2</sub> measurements at Marylebone Road (25.06.2019 to 07.10.2019) on a daily, weekly and monthly basis.

## 2.2.3 Urban background site results – Honor Oak Park

### 2.2.3.1 NO measurements

NO amount fraction measured at Honor Oak Park using the T200 ('Moly') and T200UP ('BLC') NO<sub>x</sub> analysers was between 0 and 5 nmol/mol most of time, but some peaks (up to 100 nmol/mol) were observed. The data were scaled according to the cylinder calibration factors.

The upper panel of Figure 31 shows the hourly average NO amount fractions categorised according to the day of the week. The lower left panel shows the NO amount fractions for each hour of the day, averaged across the duration of the measurement campaign. In general, the NO amount fraction remains low (< 2 nmol/mol) during the afternoon and overnight, and peaks at around 7 am each morning (5 nmol/mol on average). The plot on the lower centre panel shows the average NO amount fractions recorded in August and September and the plot on the lower right panel shows average weekday amount fractions.

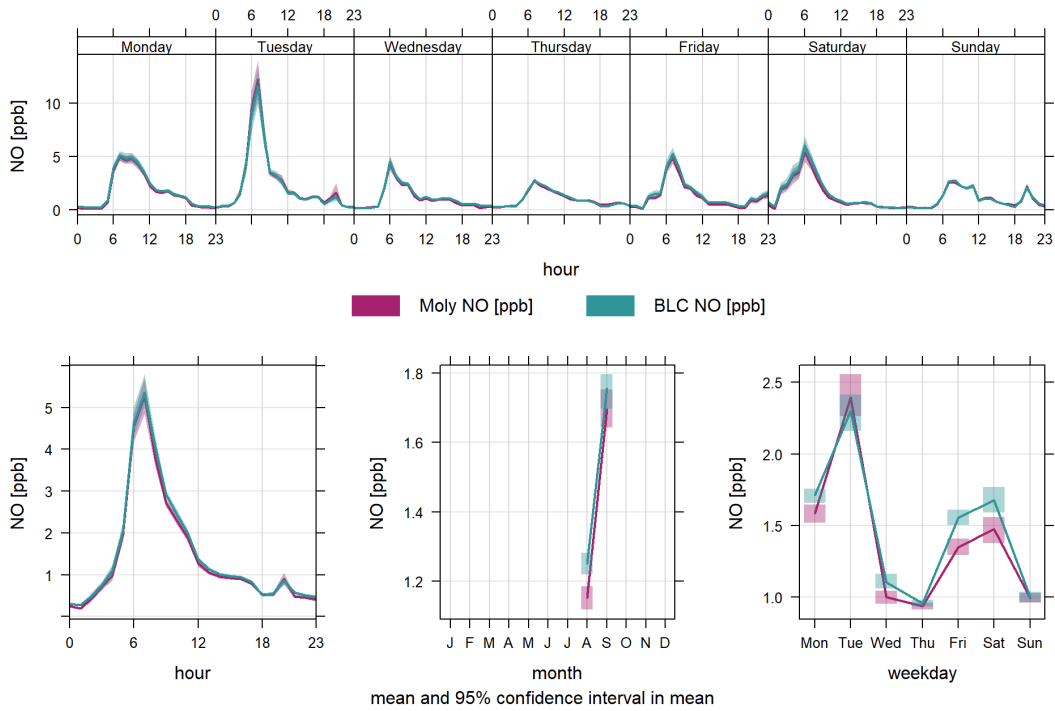


Figure 31: Ambient NO measurements at Honor Oak Park (09/08/2019 to 17/09/2019) on a daily, weekly and monthly basis.

Figure 32 and Figure 33 show the correlation in NO measurements recorded by the BLC and Moly analysers, on a 1 min and hourly basis respectively. Although there is strong overall linear relationship between the two instruments ( $R^2 = 0.99$  for hourly data), significant variation in the NO signal recorded by the two instruments is seen in the 1 min data.

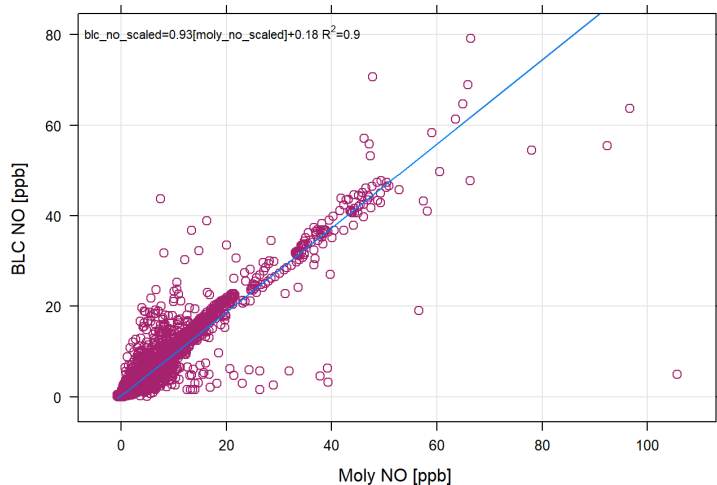


Figure 32: Comparison of NO measured using the BLC and Moly analysers (1 min data).  $y = 0.93x + 0.18$ .  $R^2 = 0.9$



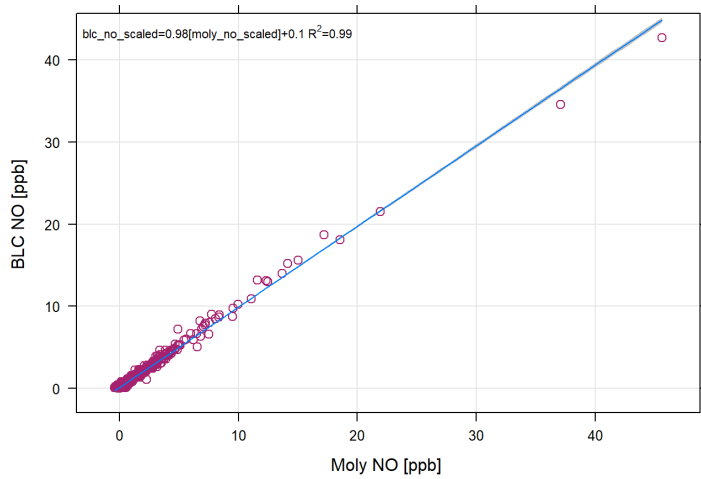


Figure 33: Comparison of NO measured using the BLC and Moly analysers (hourly data).  $y = 0.98x + 0.1$ .  $R^2 = 0.99$

Figure 34 shows the difference in the average hourly NO signals recorded by the Moly and BLC analyser, categorised according to day of the week, month, and measurement campaign. As shown in the lower left panel, over the whole campaign the NO signal recorded by the Moly analyser was approximately 50 - 300 pmol/mol lower than the BLC.

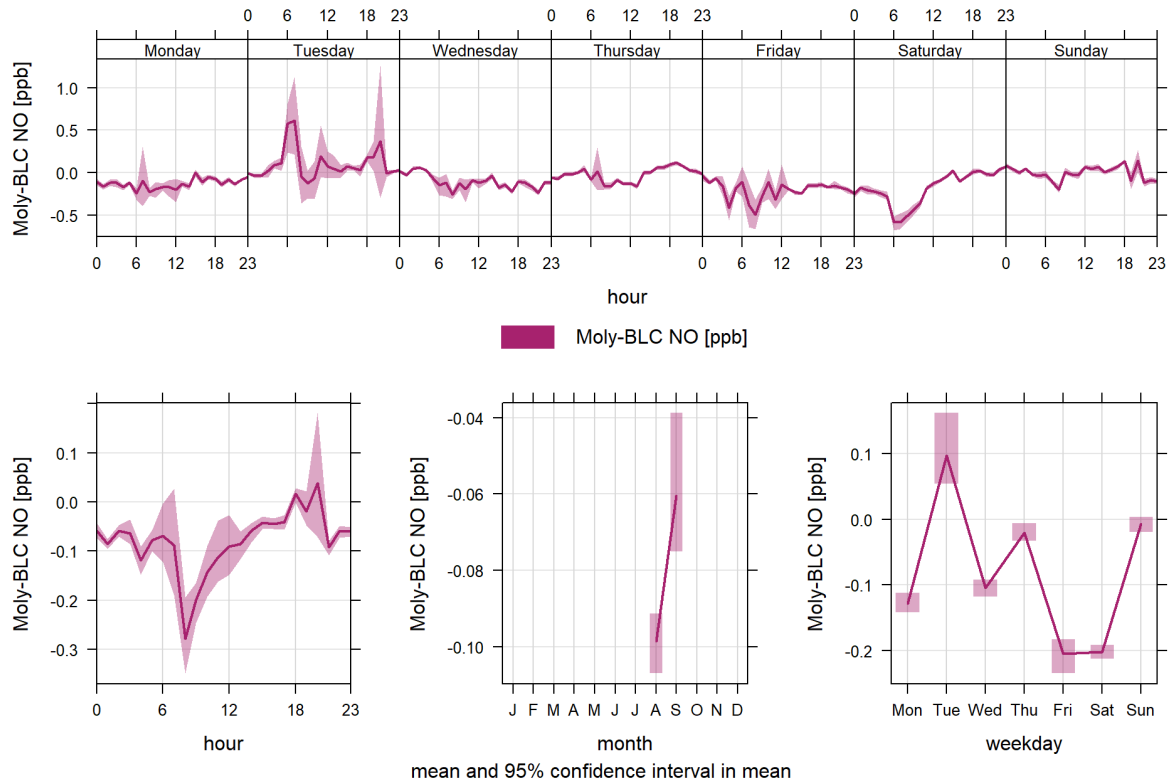


Figure 34: Absolute difference between NO measurements recorded by the Moly and BLC analyser, on a daily, weekly and monthly basis.

### 2.2.3.2 NO<sub>2</sub> measurements

Generally, NO<sub>2</sub> mixing ratios – measured at Honor Oak Park using the T500U CAPS analyser and the T200 ('Moly') and T200UP ('BLC') NO<sub>x</sub> analysers – between 0 and 15 nmol/mol were recorded, although some peaks up to 60 nmol/mol NO<sub>2</sub> were also measured. The data were scaled according to the cylinder calibration factors.

The scatter plots (Figure 35 – Figure 37) show the NO<sub>2</sub> relationships for the BLC vs Moly, CAPS vs BLC and CAPS vs Moly. Overall the NO<sub>2</sub> hourly data shows a strong linear relationship for each analyser with R<sup>2</sup> values of 0.98 - 0.99. Overall the NO<sub>2</sub> amount fraction recorded by the CAPS was slightly lower than both the BLC (CAPS = 0.98 x BLC - 0.07) and the Moly (CAPS = 0.99 x Moly - 0.23).

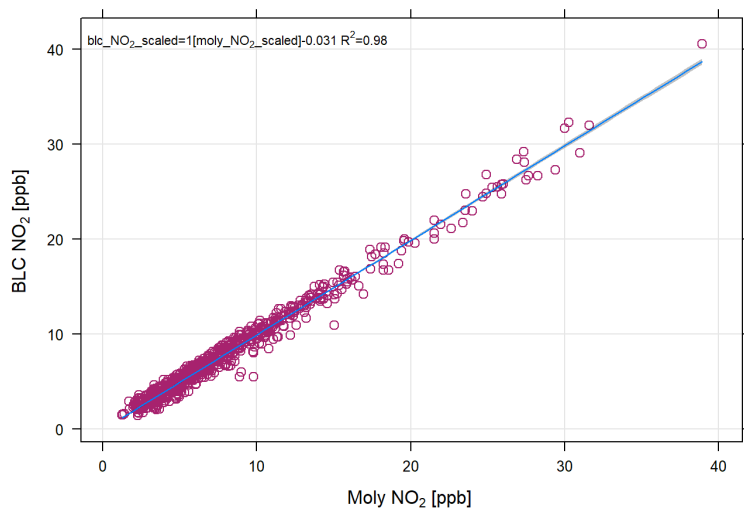


Figure 35: Comparison of NO<sub>2</sub> measured by the Moly and BLC analysers (hourly data)

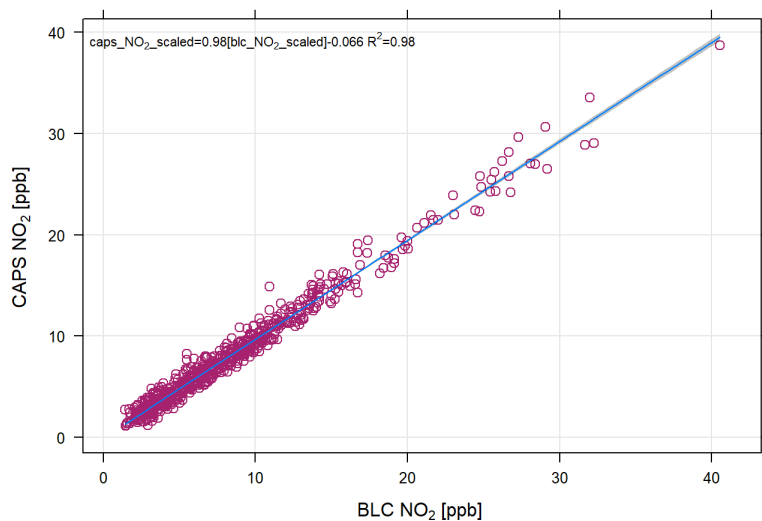


Figure 36: Comparison of NO<sub>2</sub> measured by the BLC and CAPS analysers (hourly data).

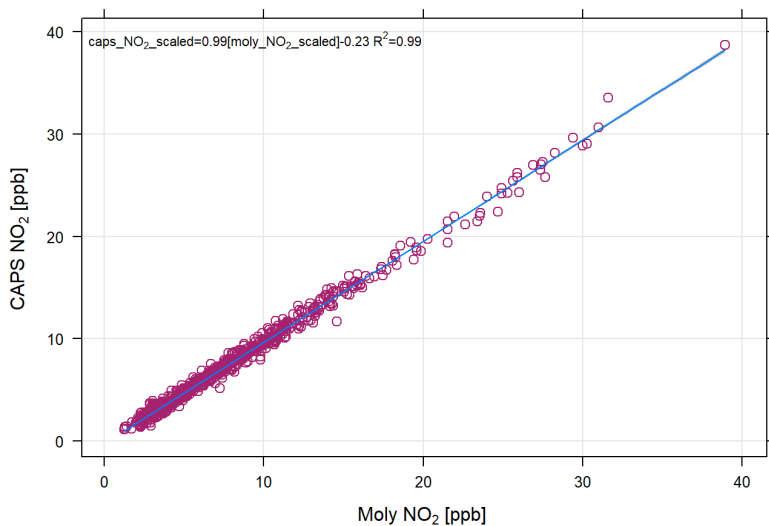


Figure 37: Comparison of NO<sub>2</sub> measured by the Moly and CAPS analysers (hourly data).

The upper panel of Figure 20 shows the hourly average NO<sub>2</sub> amount fractions for each day of the week, and the lower left panel shows the NO<sub>2</sub> amount fractions for each hour of the day, averaged across the duration of the measurement campaign. Two peaks in NO<sub>2</sub> are observed throughout the day, at approximately 6-7 am and 7-8 pm. A strong decrease in NO<sub>2</sub> amount fraction is observed after the morning peak (due to daytime photolysis) and reaches a minimum amount fraction at approximately midday. As shown in the plot on the lower centre panel, the average NO<sub>2</sub> amount fraction across the measurement period was between 7 and 9 nmol/mol. The lower right panel shows average NO<sub>2</sub> amount fractions by day of the week. Overall, the CAPS NO<sub>2</sub> analyser (direct measurement technique) recorded the lowest NO<sub>2</sub> amount fractions throughout the campaign.

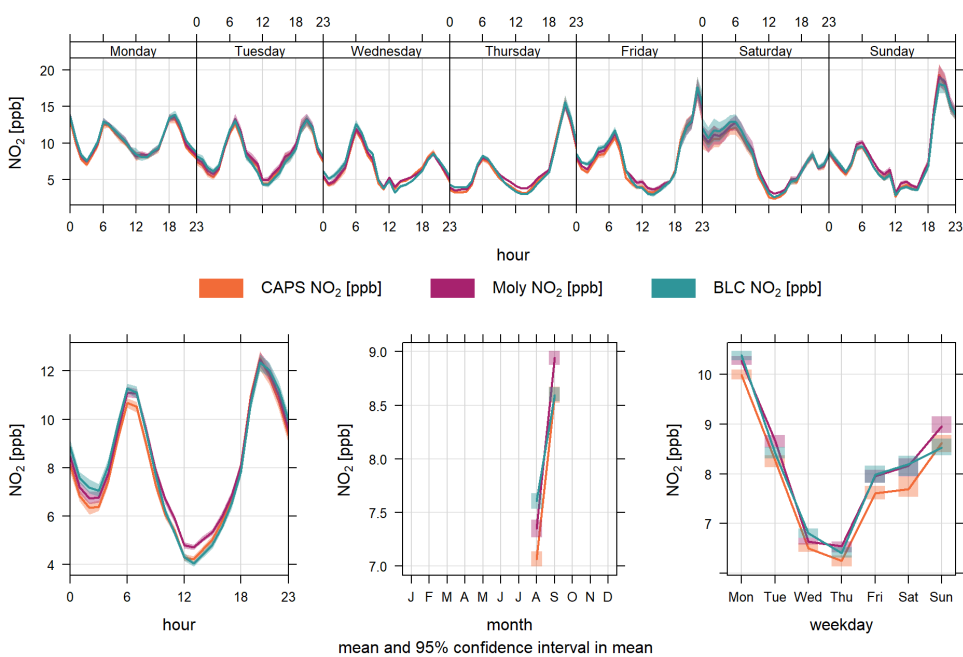


Figure 20: Ambient NO<sub>2</sub> measurements at Honor Oak Park (09/08/2017 to 17/09/2019) on a daily, weekly and monthly basis.

Figure 21 shows the difference in the average hourly NO<sub>2</sub> signals recorded by the Moly and BLC analysers throughout the measurement campaign. Although there is likely a small calibration offset, the 24-hour profile shows that the Moly NO<sub>2</sub> signal is higher than the BLC NO<sub>2</sub> signal during the day than the night. This suggests that there is some kind of daytime interference observed by the Moly analyser. Instrument comparison experiments at FZJ (A3.3.3) showed that when isobutylnitrate was added to the atmospheric simulation chamber, the Moly NO<sub>x</sub> analysers showed an interference and the BLC analysers did not.

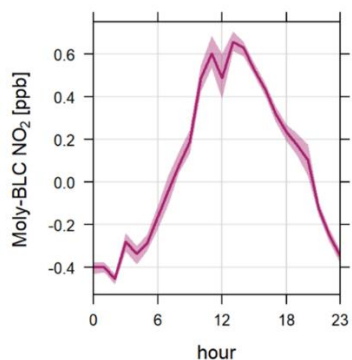


Figure 21: Absolute difference between NO<sub>2</sub> measurements recorded by the Moly and BLC analyser between 09/08/2017 and 17/09/2019.

Figure 40 shows the difference in the average hourly NO<sub>2</sub> signals recorded by the BLC and CAPS analysers throughout the measurement campaign. The BLC NO<sub>2</sub> signal is higher than the CAPS NO<sub>2</sub> signal throughout the night. This suggests that there is some kind of interference observed by the BLC analyser that is susceptible to daytime photolysis. During the experiments at FZJ (A3.3.3), isobutylnitrite was added to the chamber to simulate HONO interferences. Under dry conditions, the BLC and the CAPS did not see a NO<sub>2</sub> signal upon addition of isobutylnitrite, but under humid conditions, an interference was observed by the BLC (but not the CAPS). The results from these experiments can be seen in Figure 41 – Figure 44 (plots produced by Dr Robert Wegener, FZJ).

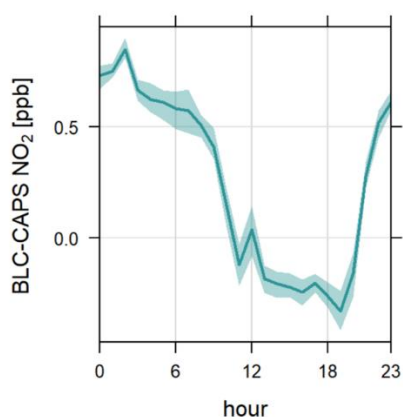


Figure 40: Absolute difference between NO<sub>2</sub> measurements recorded by the BLC and CAPS analyser between 09/08/2017 and 17/09/2019.

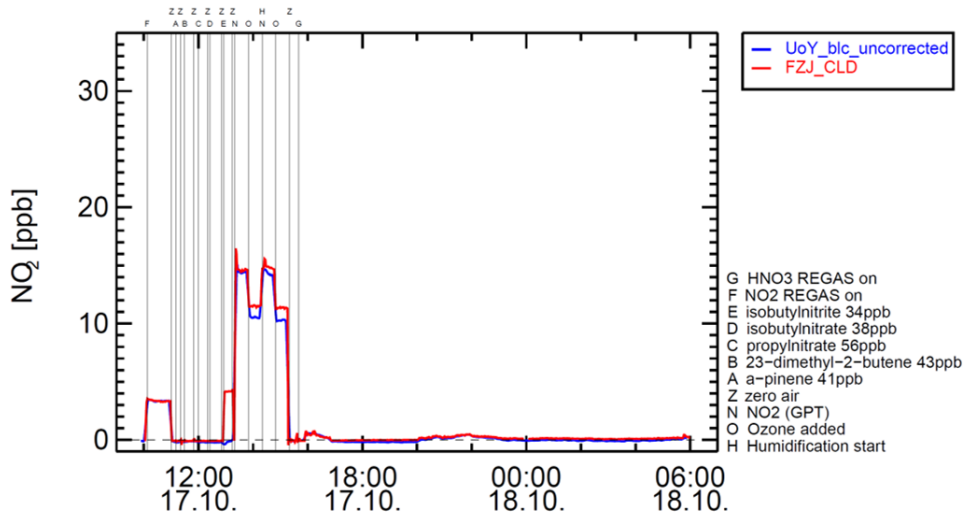


Figure 41: NO<sub>2</sub> signal recorded by the York and FZJ BLC analysers upon addition of potential interferences to the atmospheric simulation chamber under dry conditions. The addition of isobutylNitrite is at position E.

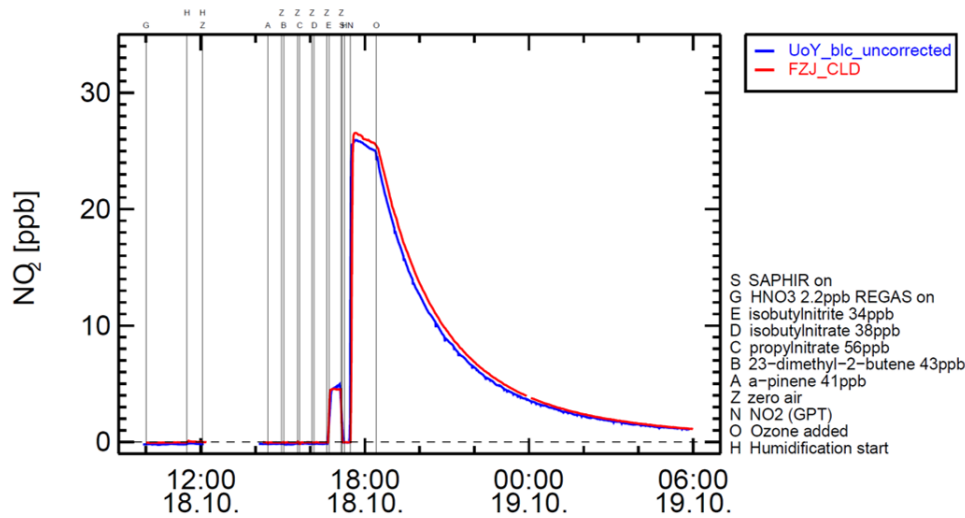


Figure 42: NO<sub>2</sub> signal recorded by the York and FZJ BLC analysers upon addition of potential interferences to the atmospheric simulation chamber under humid conditions. The addition of isobutylNitrite is at position E.

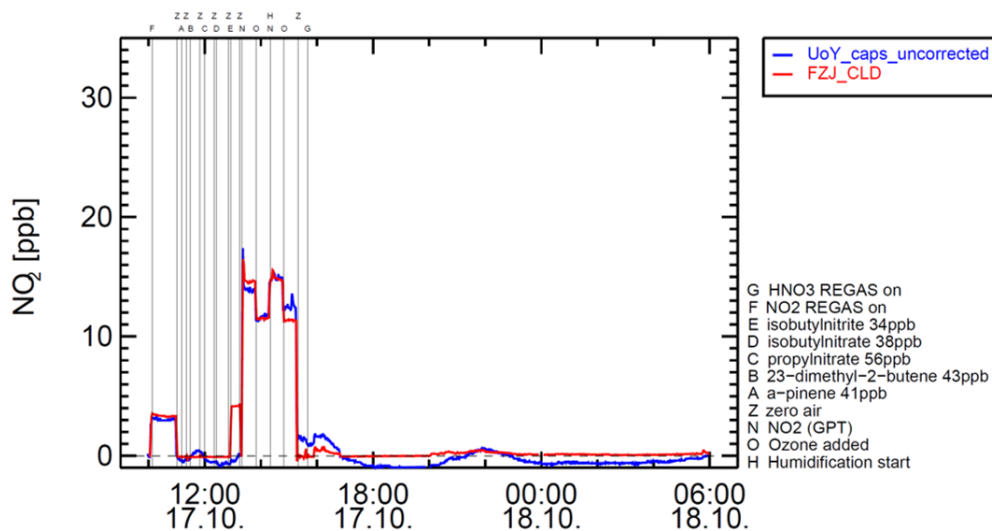


Figure 43: NO<sub>2</sub> signal recorded by the York CAPS and FZJ BLC analyser upon addition of potential interferences to the atmospheric simulation chamber under dry conditions. The addition of isobutyl nitrite is at position E.

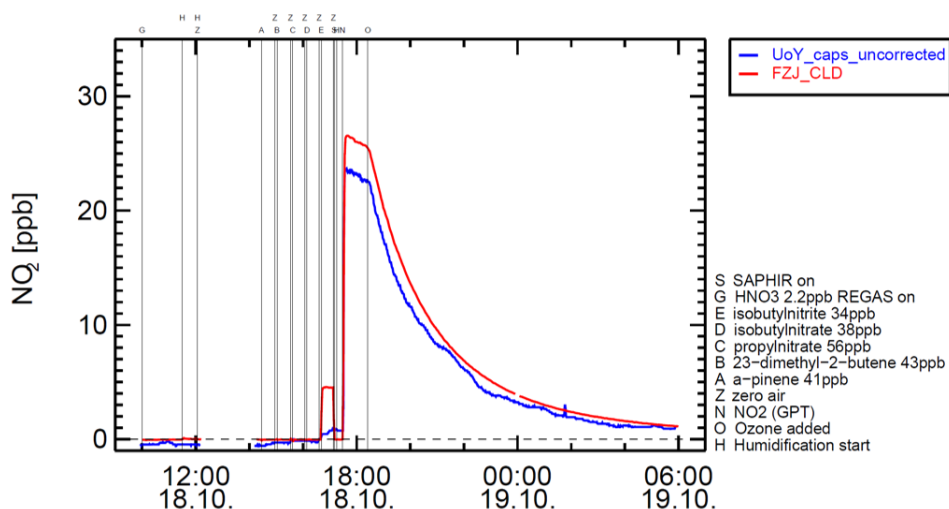


Figure 44: NO<sub>2</sub> signal recorded by York CAPS and FZJ BLC analyser upon addition of potential interferences to the atmospheric simulation chamber under humid conditions. The addition of isobutyl nitrite is at position E.

## 2.2.4 Summary

At London Honor Oak Park, the urban background site, average NO and NO<sub>2</sub> amount fractions were in the region of 0-5 and 5-15 nmol/mol respectively. Good agreement was observed between the three analysers. For NO<sub>2</sub>, the measurements obtained by the two CLDs (indirect method) were slightly higher than the signal measured by the CAPS analyser (direct method). The increased NO<sub>2</sub> signals for the Moly and BLC analysers appeared to depend on the time of day and possible interfering compounds were identified.

At Marylebone Road, the urban traffic site, average NO and NO<sub>2</sub> amount fractions were considerably higher (several hundred nmol/mol) and significant variation in the signals was observed. This site is associated with fresh NO<sub>x</sub> emissions from nearby traffic, unlike Honor Oak Park where air masses are

likely to be more aged and representative of urban background levels. At Marylebone Road, the CAPS NO<sub>2</sub> signal was ‘compressed’ compared to the signal from the CLD’s and showed significantly less variation. Both CLDs reported higher NO<sub>2</sub> amount fractions than the CAPS analyser and the BLC signal was higher than the Moly. These differences may be a result of the inherent differences in the instrument measurement technique or due to a problem with the internal pump inside the CAPS analyser, which may not be adequate for sampling from an inlet that is located several metres away from the instrument.

**Acknowledgements:** York - Will Drysdale and James Lee; KCL - Anja Tremper, David Green, Ana Beckett, Max Priestman, Stefan Gillot.

## 2.3 Comparison 3 – A2.3.4 outputs

In activity A2.3.4, dynamic reference standards were generated by using a portable generator based on permeation (A2.1.3) and applied to two air quality monitoring sites (see Table 33). The effects on data quality of using dynamic reference standards, compared to traditional static NO reference standards, were assessed. For that purpose, the overall uncertainty of the direct NO<sub>2</sub> measurement – taking into account the associated uncertainty of the new reference standards – was evaluated.

Table 33: List of sites and instruments used in comparison 4

Site	Site type	Number of instruments	Instruments type
Dübendorf (CH)	suburban	4	CAPS (1), CLD (1), QCLAS (2)
Hohenpeissenberg (DE)	rural	2	CAPS (1), CLD (1)

### 2.3.1 Empa results

The results for this comparison are included 2.1.1 *Empa results* within 2.1 *Comparison 1 – A2.3.1 outputs*.

### 2.3.2 DWD results

(Author: Annika Kuß, DWD)

DWD compared the currently applied calibration concept using gas phase titration of NO, i.e. traceability to static reference standards for NO, to the dynamic reference standards generated using METAS portable generator based on permeation and dilution and a permeation device calibrated with a magnetic suspension balance.

### 2.3.2.1 Experimental setup

The comparison took place at the monitoring station of Hohenpeissenberg (DE) during a two-week measurement period in November 2019. Four calibrations of two NO<sub>2</sub> instruments based on different measurement principles were performed during this period. For the calibration, two different methods were used: one based on the standard calibration procedure using gas phase titration and one based on standard dynamic generation combining permeation and dilution procedures.

#### NO<sub>2</sub> instruments

A chemiluminescence instrument (CLD) coupled with a photolytic converter was used to quantify NO and NO<sub>2</sub>. The Blue Light NO<sub>2</sub> Converter (Teledyne-API) was applied in combination with the ECO PHYSICS CLD 770 AL pmol/mol. The photolytic reaction takes place in a reaction cell where the gas is being exposed to light at a specific wavelength range (380 nm – 420 nm) from an LED array, which causes the conversion of NO<sub>2</sub> to NO.

For direct NO<sub>2</sub> detection, an Aerodyne CAPS NO<sub>2</sub> Monitor (based on the measurement principle of cavity attenuated phase shift) has been used, which provides a direct absorption measurement of nitrogen dioxide at 450 nm in the blue light region of the electromagnetic spectrum. Unlike standard chemiluminescence-based monitors, this instrument requires no conversion of NO<sub>2</sub> to another species. Data of 1 minute time resolution was recorded/analysed with a level of detection (3σ noise levels) of less than 100 parts per trillion. This monitor used NO<sub>2</sub>-free air (filtered pure air) for periodic automated baseline measurements every two hours. During some periods of the NO<sub>2</sub> generations for this report, the automated zeroing was turned off.

### 2.3.2.2 Calibration using gas phase titration of NO

Four calibrations of DWD's selective and direct NO<sub>2</sub> instruments have been performed during the two-week measurement period in November 2019 via the standard calibration procedure using gas phase titration.

The calibration unit AnSYCO SYCOS K-GPT-DLR has been used to run the standard calibration, which is operationally being used for weekly NO and NO<sub>2</sub> calibrations. The calibration procedure is based on the dilution of a standard NO gas mixture and gas phase titration based on the reaction of O<sub>3</sub> with NO to NO<sub>2</sub>. As the current working standard a nitric oxide in nitrogen cylinder D0417RC by NPL with a amount fraction of 10.05 μmol/mol ± 0.2 μmol/mol is used, which yields a target volume mixing ratio of 31.17 nmol/mol for the standard span checks.

Regularly the analyser are being calibrated by purified air, followed by a span NO volume mixing ratio of around 30ppb and finally the titration of NO + O<sub>3</sub> → NO<sub>2</sub> + O<sub>2</sub>. Ozone is added to the NO in deficit. Therefore, the difference of NO measured with and without conversion by the CLD instrument can be used as reference to calibrate the CAPS monitor. The calibrations including the calibration factors are summarised below in Table 34. During the calibrations on the 11<sup>th</sup> and the 18<sup>th</sup> of November 2019 both DWD's instruments were calibrated contemporaneously, while on the 4<sup>th</sup> and the 6<sup>th</sup> of November 2019, the CAPS instrument was calibrated directly after the chemiluminescence detector. In that case, the zero followed the span measurement during the CAPS calibration. Since CAPS was calibrated here right after the CLD, this difference between the amount



fractions of both Instruments leads back to the NO<sub>2</sub> amount fraction not being sufficiently stable yet and yields to a measured mole fraction of 1-3% greater than the results measured within the timeframe before during the CLD calibration. The volume mixing ratio of NO<sub>2</sub> measured by the CLD instrument calculates from the difference of NO converted (NO.c) and the actual NO measured

$$NO_2 = \frac{(NO.c - NO)}{conv.Efficiency}$$

and the

$$conv. Efficiency = 1 - \frac{NO.c(1) - NO.c(2)}{NO(1) - NO(2)}$$

with (1)=before addition of ozone and (2)=during addition of ozone

The average conversion efficiency of the CLD instrument evolves to 75.67 ± 0.55 %. While an average calibration coefficient 0.982 ± 0.013 was calculated for the CAPS monitor with a relative precision of 0.1 %.

Table 34: CLD and CAPS NO<sub>2</sub> calibration via gas phase titration of NO + Ozone using the calibration unit SYCOS (The standard deviation of the single measured amount fractions are given in brackets.)

Date of calibration	CLD				CAPS	
	remaining NO [nmol/mol]	NO.c [nmol/mol]	conversion Efficiency [%]	NO <sub>2</sub> [nmol/mol]	NO <sub>2</sub> zerocorr. Uncalibrated [nmol/mol]	cal.coeff. [nominal/signal]
04/11/2019	15.200 (0.019)	27.378 (0.019)	<b>0.750</b>	<b>16.236</b>	<b>16.544</b> <b>(0.015)</b>	<b>0.981</b>
06/11/2019	15.110 (0.063)	27.457 (0.092)	<b>0.764</b>	<b>16.171</b>	<b>16.829</b> <b>(0.023)</b>	<b>0.961</b>
11/11/2019	15.144 (0.012)	27.629 (0.036)	<b>0.761</b>	<b>16.415</b>	<b>16.514</b> <b>(0.015)</b>	<b>0.994</b>
18/11/2019	15.039 (0.007)	27.283 (0.028)	<b>0.753</b>	<b>16.265</b>	<b>16.383</b> <b>(0.013)</b>	<b>0.993</b>

### 2.3.2.3 Calibration using a permeation-based portable generator

In addition to the standard calibration procedure (gas phase titration) being used at the air monitoring station Hohenpeissenberg, a variety of NO<sub>2</sub> amount fractions originating from the ReGaS1 device have been set to verify the stability and reproducibility of the new dynamic standard on DWD's NO<sub>2</sub> analysers. The NO<sub>2</sub> permeation tube NO<sub>2</sub>\_W\_400\_025 was provided by METAS who carried out its calibration before and afterwards to determine the permeation rate of the permeation source (see 2.1.1.1 *Experimental setup – Calibration methods*). All generated mole fractions are shown in Table 35. The same nominal NO<sub>2</sub> mole fractions (ReGaS1) versus the measured (CLD and CAPS) are plotted in Figure 45. The CLD also detected a slight impurity of NO inside the NO<sub>2</sub> permeation source. The ReGas1 NO<sub>2</sub> dynamic dilution system was quantified for NO using the CLD device. Due to the deviation of the DWD calibration and the ReGas1 amount fraction,

the data was normalised to the measured CLD NO<sub>2</sub> amount fraction. The NO impurity was determined to be (< 0.3 % ± 0.05 %), which correlates and increases with elevating ReGaS1 generated mole fractions. These mole fractions are also shown (orange) in the figure. The detection limit of the CLD NO is 30 pmol/mol (1 min, 2 sigma). Most experiments were operated simultaneously on both analysers. Two out of six amount fractions were repeated, as 19.8 nmol/mol (on 11/11/2019 and 18/11/2019) and 43.5 nmol/mol (on 08/11/2019 and 18/11/2019) which were used for reproducibility checks.

Table 35: NO<sub>2</sub> amount fraction generated by ReGaS1 – measured amount fractions of Chemiluminescence Detector (CLD) and CAPS Monitor. The standard deviation of the single measured amount fractions, the uncertainty of the ReGaS1 data and the errors propagation for the derived ratios are given in brackets.

ReGaS1 NO <sub>2</sub>			CLD			CAPS	
NO <sub>2</sub> [nmol/mol]	cover factor k	Dilution Steps	NO <sub>2</sub> [nmol/mol]	NO [nmol/mol]	NO <sub>2</sub> /ReGaS1 (cal.factor)	NO <sub>2</sub> [nmol/mol]	NO <sub>2</sub> /ReGaS1 (cal.factor)
46.65 (0.66)	2	dil1				47.879 (0.028)	1.026
47.08 (0.67)	2	dil1	47.048 (0.087)	0.208 (0.005)	0.999		
66.12 (0.92)	2	dil1	66.726 (0.130)	0.258 (0.004)	1.009		
66.03 (0.92)	2	dil1				66.640 (0.020)	1.009
92.2 (1.3)	2	dil1				96.007 (0.019)	1.041
43.49 (0.61)	2	dil2	43.730 (0.404)	0.200 (0.004)	1.006	43.774 (0.382)	1.007
10.62 (0.29)	2	dil1	10.371 (0.178)	0.088 (0.035)	0.977	10.178 (0.088)	0.958
19.79 (0.29)	2	dil2	19.548 (0.050)	0.130 (0.004)	0.988	19.848 (0.014)	1.003
43.49 (0.61)	2	dil1	45.314 (0.283)	0.198 (0.004)	1.042	46.544 (0.251)	1.070
19.83 (0.29)	2	dil2	20.433 (0.036)	0.137 (0.003)	1.030	20.429 (0.015)	1.030
<b>Average:</b>					<b>1.0073 (0.021)</b>		<b>1.018 (0.031)</b>

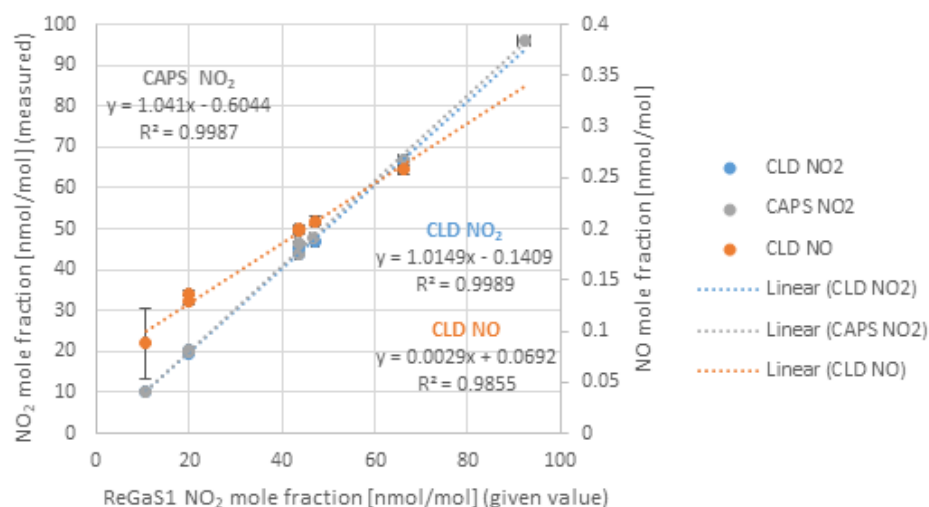


Figure 45: ReGaS1 (given NO<sub>2</sub> amount fraction) versus measured on CLD NO<sub>2</sub> (blue), CLD NO (orange) and CAPS (grey)

#### 2.3.2.4 Uncertainty budget

The uncertainty budget of the two different calibration methods were calculated by the uncertainty of the MFCs ( $U(2\sigma) = 1.4\%$ ), the uncertainty of the cylinder amount fraction (Air Liquide NO  $U(2\sigma) = 2.5\%$ ), the reproducibility of the CLD NO<sub>2</sub> converter efficiency (3.8 %) and the reproducibility of the CAPS sensitivity (4.6 %).

### 3 Recommendations

Based on the results from Task 2.3 of the project MetNO<sub>2</sub>, we recommend the following guidelines on the use of static and dynamic gas standards at monitoring stations for the calibration of field instrumentation.

#### 3.1 Measuring method

Choosing the appropriate analyser is an essential part of the measuring process to obtain accurate NO<sub>2</sub> amount fraction values. In Task 2.3 of the project MetNO<sub>2</sub> different chemiluminescence detector (CLD) analysers – accepted indirect method for NO<sub>2</sub> monitoring sites – were compared to direct methods such cavity attenuated phase shift spectrometers (CAPS) and quantum cascade laser absorption spectrometers (QCLAS).

##### o Direct analysers as recommended NO<sub>2</sub> measuring method at suburban and urban background sites

Although results from rural, suburban and urban background sites (Hohenpeissenberg, Dübendorf, Honor Oak Park) showed a good agreement between direct and indirect methods for NO<sub>2</sub> measurements, overall the direct methods (CAPS and QCLAS) appears to be most suitable for deployment at urban background and suburban sites.

The direct NO<sub>2</sub> measuring methods (e.g. CAPS) are suitable for this type of sites because the NO<sub>2</sub> levels are relatively low and stable. Furthermore, the use of a direct measurement technique is important because the air masses are more likely to be aged and the proportion of total NO<sub>y</sub> that is comprised of NO<sub>2</sub> compounds is likely to be higher. This means that the use of NO<sub>2</sub> analysers that suffer from potential interferences should be avoided as it may lead to an overprediction in the amount fraction of NO<sub>2</sub>; this is likely to introduce a more significant error in the reported NO<sub>2</sub> amount fraction at locations where absolute NO<sub>2</sub> amount fractions are lower and air masses are more aged.

In the urban site (Marylebone Road), associated with fresh NO<sub>x</sub> emissions from nearby traffic, the CLD readings were higher than the CAPS readings, which showed compressed signals and less variation. These differences may be a result of the inherent differences in the instrument measurement technique or due to a problem with the internal pump inside the CAPS analysers, which may not be adequate for sampling from an inlet that is located several metres away from the

instrument. This lack of agreement suggest that further tests are needed to establish the optimum setup for measuring NO<sub>2</sub> at urban traffic sites.

- Simultaneous measurements of NO and NO<sub>y</sub>

It is recommended that simultaneous measurements of NO and NO<sub>y</sub> are carried out, as is the current set up at Honor Oak Park (see 2.2.3 *Urban background site results – Honor Oak Park*).

## 3.2 Calibration method

Instrument calibration is another essential part of the measuring process to obtain accurate NO<sub>2</sub> amount fraction values. Accurate, reliable and traceable monitoring results are crucial for data analysis, particularly when the results are part of air quality monitoring networks.

The calibration of NO<sub>2</sub> analysers established the relationship between instrument readings and known NO<sub>2</sub> amount fractions. In addition, instrument calibration at regular intervals is needed to compensate for baseline and span drift of the instrument and to check the linearity of the instrument response.

In Task 2.3 of the project MetNO<sub>2</sub> several calibration methods were applied to the different instruments, assessing reference standard effects on NO<sub>2</sub> data quality (i.e. repeatability and accuracy). Calibrations using static NO reference standard and gas phase titration were compared with those using NO<sub>2</sub> static and dynamic reference standards.

- PFA or coated stainless steel as recommended material for tubing

In order to reduce negative impacts on the calibration process, resulting from the reactivity of NO<sub>2</sub> with surfaces, the use of PFA or coated (e.g. SilcoNert 2000) stainless steel tubing is highly recommended. Both materials are relatively inert to NO<sub>2</sub>, which minimises the adsorption of NO<sub>2</sub> molecules by the tubing surface and in turn memory effects.

- Synthetic air or nitrogen as recommended dilution air

We recommend using a dilution air as free of analyte and interfering species as possible, especially for those calibration methods that required dilution of the reference standard. Good options for the calibration of NO<sub>2</sub> analysers are synthetic air or nitrogen with a 6.0 quality (99.99990 % purity). The use of gas purifiers to remove residual water is highly recommended, if dilution air with quality 6.0 is not available. Low amount fractions of water will reduce the formation of HNO<sub>3</sub>, HONO and related species in the resulting reference gas mixture.

- Determination of impurities within reference standards

The determination of impurities within reference standards used for the instrument calibration is vital to ensure complete and realistic uncertainty budget of the calibration. This uncertainty is part of the overall uncertainty of the measurements. Therefore, the identification and quantification of impurities within reference standards is a needed step to achieve comparable, traceable and accurate results.

Recommendations on the selection and use of methods to determine impurities in reference standards, together with the description of most common impurities identified in reference standards can be found in deliverable D3: *"Description of the techniques for the determination of major impurities in NO<sub>2</sub> reference standards, with recommendations for impurity analysis and methods to suppress their formation"*.

#### ○ Determination of the instrument stabilization period

Before setting up the calibration protocol for the used instruments, an important step is determining the stabilization period of the instrument for the calibration method selected. As shown by results in 2.1.1.2 *Calibration data – Stabilization period*, this period can go from 1.5 hours to up 10 hours for the same instrument. This is especially important when using dynamic reference standards based on permeation. In this case, the stabilization period of the permeation device should also be determined.

The stabilization period should be respected. Only data recorded after this period should be considered for the instrument calibration.

#### ○ Periodic calibration of the elements involved in the calibration process

When using external elements to dilute static reference standards (e.g. mass flow controllers (MFMs)), these elements should be recalibrated with the recommended periodicity for such element (e.g. periodicity for MFMs every two years). Preferably, traceable references should be used to ensure an unbreakable chain of calibrations for the element.

Periodic calibrations are especially important when using dynamic reference standards, such as the one described in this guide. Apart from the calibration of the generator internal elements, the periodic calibration of the permeation unit (every 6 months maximum) is critical to ensure accurate and stable reference standards. This recalibration can entail important costs for monitoring sites, which should estimate and compare budget differences generated by using dynamic vs. static reference standards. Avoiding the periodic calibration of the permeation unit, for example, can lead to differences in the relative uncertainty of the reference gas mixtures up to 2 %.

#### ○ Calibration method recommendations for NO<sub>2</sub> instruments

Results from section 2.1 *Comparison 1 – A2.3.1 and A2.3.3 outputs* show that calibrations performed using the [newly developed static reference standards \(1 µmol/mol\)](#) have relatively high

expanded uncertainties (4.0 – 5.8 %). The results suggest also that these cylinders may have issues associated with surface effects and temporal stability. This is especially true in section 2.1.3 (calibration of indirect instruments using the new static standards). The poor stability of the amount fraction over time of all cylinders and the large differences between NO<sub>2</sub> measured in cylinders and the certified value suggest that calibrations performed with traceable and certified NO<sub>2</sub> cylinders would not be suitable for traceable calibrations of instrumentation in the field.

Although the stability and differences in amount fraction compared to the certified value might be explained by one-off rapid changes in the NO<sub>2</sub> amount fractions soon after certification or during field installation, other reasons might explain them. For example, NO<sub>2</sub> losses in regulators and pipework or high amount fractions of NO<sub>2</sub> in the test cylinders outside the usual operating levels of the instrument and linear calibration range.

Regarding the use of [dynamic reference gas standards](#) (i.e. permeation + dilution) to calibrate NO<sub>2</sub> instruments, recommendations cannot be done only with the results presented in section 2.3 *Comparison 3 – A2.3.4 Outputs*. Although results from A2.2.1 suggest that performing calibrations using dynamic standards can result in relative high calibration uncertainty values, this is not so clear in results from A2.3.2. One of the main limitations of this calibration method is the long time required for stabilization of the permeation unit membrane when starting a new generation or changing the parameters of the generator (up to several hours). Other limitation is the need of periodic recalibration of the permeation units. To ensure the traceability of the calibration standards, these should be done by sending the permeation unit to a NMI or DI (in most cases, several weeks). Despite these limitations, using the system following the required steps and conditions can generate reference standards at low amount fractions < 100nmol/mol and relatively low uncertainties (< 3 %). Some of the requirements are periodic recalibration of the permeation unit (twice or three times per year), respecting the lifetime of the permeation units (ca. 20 months), recalibration of the generator every two weeks, respecting the stabilization period...

Therefore, results presented in section 2 suggest that further improvements in NO<sub>2</sub> reference standards are required before they can displace the traditional gas phase titration of NO reference standards with ozone to make in-situ NO<sub>2</sub> reference standards.

### 3.3 Evaluation of measurement uncertainty

The calculation and evaluation of measurement uncertainty is essential to assess the reliability of the measured NO<sub>2</sub> amount fractions and to be able to compare measurement results. Furthermore, this uncertainty allows knowing the confidence that can be placed in any decisions based on the measured values.

#### ○ Calculation of complete uncertainty budgets of the reference standards used for the instrument calibration

There are several aspects that should be considered to calculate the overall uncertainty of the measurements. An important contribution to the measurement uncertainty is the uncertainty of the instrument calibration. Therefore, special care should be taken to elaborate complete uncertainty budget of the calibration process, mainly the reference standards. The contribution to the overall

measurement uncertainty will differ depending on the reference standards used for the instrument calibration.

According to results from *2.1.1.3 Ambient air measurements – measurement uncertainties*, most of the overall uncertainty of the performed NO<sub>2</sub> measurements using NO<sub>2</sub> static reference standard as calibration method is due to the relatively high uncertainty on the NO<sub>2</sub> amount fraction in the gas cylinder (90 % contribution to the overall uncertainty). The uncertainty of the reference standard (4 %, k = 2) is mostly due to the impurities content in the cylinder and the temporal stability of the gas. The uncertainty contribution of the dilution gas (purity) and mass flow controllers regulating the dilution flow (if used) should be considered. When using the standard calibration method (NO standard + GPT), the calibration uncertainty represents only 10 % of the overall uncertainty and is mainly due to the uncertainty of the NO amount fraction in the gas cylinder (1 %, k = 2). For this calibration method, uncertainty of the conversion efficiency should also be included in the uncertainty budget of the calibration. Regarding the dynamic method used in this experiment, the main contribution to the calibration uncertainty is the temporal stability of the permeation unit (94 %), followed by uncertainty of the permeation device calibration (5 %) and uncertainty of the dilution flow (0.4 % for one-step dilution; 1 % for two-step dilution). The high contribution of the permeation unit stability is mostly due to the lack of recalibration, resulting in a rough estimation of the permeation rate after almost 10 months from its calibration. As mentioned in *3.2 Calibration method*, periodic calibrations may help to reduce this uncertainty.

Comparing the uncertainty values described above for the dynamic calibration method with the uncertainty budget used in *2.4.2 DWD results* (complete uncertainty budget not shown), the main contribution to the calibration uncertainty is the purity of the permeation device (34 %). Other contributors to the uncertainty are the temporal stability of the permeation unit (16 %), the dilution flow (depending on the flow used between 4 % and 8 % for one-step dilutions and around 10 % for two-step dilutions) and the temperature variation of the permeation device within the oven (1 %). To reduce this uncertainty, the identification and quantification of impurities within the permeation unit should be performed, as mentioned in *3.2 Calibration method*.

#### ○ Inclusion of data correction uncertainties in the overall uncertainty budget of the measurement

Another important element that should be included in the overall uncertainty budget is data correction uncertainties. Some of the data corrections to be considered are instrument drift, reactions in the sampling line of compounds that might influence the read values of the instrument (e.g. NO + O<sub>3</sub> reaction) and interferences between compounds, among others.

## References

- Bernard, S.M., Samet, J.M., Grambsch, A., Ebi, K.L., Romieu, I. (2001). The potential impacts of climate variability and change on air pollution-related health effects in the United States. *Environmental Health Perspectives*, 109, 199–209. <https://doi.org/10.2307/3435010>
- Carslaw, D.C., Beevers, S.D. (2004). Investigating the potential importance of primary NO<sub>2</sub> emissions in a street canyon. *Atmospheric Environment*, 38, 3585–3594. <https://doi.org/10.1016/j.atmosenv.2004.03.041>
- Casquero-Vera, J.A., Lyamani, H., Titos, G., Borrás, E., Olmo, F.J., Alados-Arboledas, L. (2019). Impact of primary NO<sub>2</sub> emissions at different urban sites exceeding the European NO<sub>2</sub> standard limit. *Science of the Total Environment*, 646, 1117–1125. <https://doi.org/10.1016/j.scitotenv.2018.07.360>
- Dunlea, E.J. (2007). Evaluation of nitrogen dioxide chemiluminescence monitors in a polluted urban environment. *Atmospheric Chemistry and Physics*, 7, 2691–2704. <https://doi.org/10.5194/acp-7-2691-2007>
- EEA (2018). European Environment Agency. *Europe's urban air quality – re-assessing implementation challenges in cities*. EEA Report, No 24/2018. <https://www.eea.europa.eu/publications/europes-urban-air-quality>
- EEA (2019). European Environment Agency. *Air quality in Europe – 2019 report*. EEA report, No 10/2019. <https://www.eea.europa.eu/publications/air-quality-in-europe-2019>
- ETC/ACM (2013). European Topic Centre on Air Pollution and Climate Change Mitigation. *Air Implementation Pilot – Assessing the modelling activities*. ETC/ACM Technical Paper 2013/4.
- Flores, E., Idrees, F., Moussay, P., Viallon, J., Wielgosz, R., Fernández, T., Ramírez, S., Rojo, A., Shinji, U., Waldén, J., Sega, M., Sang-Hyub, O., Macé, T., Couret, C., Qiao, H., Smeulders, D., Guenther, F.R., Thorn III, W.J., Tshilongo, J., Godwill Ntsasa, N., Štovčík, V., Valková, M., Konopelko, L., Gromova, E., Nieuwenkamp, G., Wessel, R.M., Milton, M., Harling, A., Vargha G., Tuma, D., Kohl, A., Schulz, G. (2012a). Final report on international comparison CCQM-K74: Nitrogen dioxide, 10 µmol/mol. *Metrologia*, 49 (1A), 08005.
- Flores, E., Viallon, J., Moussay, P., Idrees, F., Wielgosz, R.I. (2012b). Highly accurate nitrogen dioxide (NO<sub>2</sub>) in nitrogen standards based on permeation. *Analytical Chemistry*, 84 (23), 10283-10290.
- Hughes, E.E., Rook, H.L., Deardorff, E.R., Margeson, J.H., Fuerst, R.G. (1977). Performance of a nitrogen dioxide permeation device. *Analytical Chemistry*, 49, 1823-1829, 1977.
- Kley, D. and McFarland, M. (1980). Chemiluminescence detector for NO and NO<sub>2</sub>. *Atmospheric Technology*, 12, 63–69.
- Lai, H.-K., Hedley, A.J., Thach, T.Q., Wong, C.-M. (2013). A method to derive the relationship between the annual and short-term air quality limits – analysis using the WHO Air Quality Guidelines for health protection. *Environmental International*, 59, 86–91. <https://doi.org/10.1016/j.envint.2013.05.013>
- Latza, U., Gerdes, S., Baur, X. (2009). Effects of nitrogen dioxide on human health: systematic review of experimental and epidemiological studies conducted between 2002 and 2006. *International Journal of Hygiene and Environmental Health*, 212, 271–287. <https://doi.org/10.1016/j.ijheh.2008.06.003>
- Lerdau, M.T., Munger, J.W., Jacob, D.J. The NO<sub>2</sub> flux conundrum. *Science*, 289, 2291–2293. <https://doi.org/10.1126/science.289.5488.2291>
- Malley, C.S., von Schneidmesser, E., Moller, S., Braban, C.F., Hicks, W.K., Heal, M.R. (2018). Analysis of the distributions of hourly NO<sub>2</sub> concentrations contributing to annual average NO<sub>2</sub> concentrations across the



European monitoring network between 2000 and 2014. *Atmospheric Chemistry and Physics*, 18, 3563–3587. <https://doi.org/10.5194/acp-18-3563-2018>

Mazurenka, M., Wada, R., Shillings, A.J.L., Butler, T.J.A., Beames, J.M., Orr-Ewing, A.J. (2005). Fast Fourier transform analysis in cavity ring-down spectroscopy: application to an optical detector for atmospheric NO<sub>2</sub>. *Applied Physics B: Lasers and Optics*, 81, 135–141. <https://doi.org/10.1007/s00340-005-1834-1>

Patimisco, P., Scamarcio, G., Tittel, F.K., Spagnolo, V. (2014). Quartz-enhanced photoacoustic spectroscopy: a review, *Sensors*, 14, 6165–6206. <https://doi.org/10.3390/s140406165>

Richter, A., Burrows, J.P., Nuß, H., Granier, C., Niemeier, U. (2005). Increase in tropospheric nitrogen dioxide over China observed from space. *Nature*, 437, 129–132. <https://doi.org/10.1038/nature04092>

Ridley, B.A. and Howlett, L.C. (1974). An instrument for nitric oxide measurements in the stratosphere. *Review of Scientific Instruments*, 45, 742–748. <https://doi.org/10.1063/1.1686726>

Robinson, E. and Robbins, R.C. (1970). Gaseous nitrogen compound pollutants from urban and natural sources. *Journal of Air Pollution Control Association*, 20, 303–306. <https://doi.org/10.1080/00022470.1970.10469405>

Ryerson, T.B., Williams, E.J., Fehsenfeld, F.C. (2000). An efficient photolysis system for fast – response NO<sub>2</sub> measurements. *Journal of Geophysical Research*, 105, 26447–26461, <https://doi.org/10.1029/2000JD900389>

Sirtori, C. and Nagle, J. (2003). Quantum Cascade Lasers: the quantum technology for semiconductor lasers in the mid-far-infrared. *Comptes Rendus Physique*, 4, 639–648. [https://doi.org/10.1016/S1631-0705\(03\)00110-5](https://doi.org/10.1016/S1631-0705(03)00110-5)

Steinbacher, M., Zellweger, C., Schwarzenbach, B., Bugmann, S., Buchmann, B., Ordóñez, C., Prevot, A.S.H., Hueglin, C. (2007). Nitrogen oxide measurements at rural sites in Switzerland: bias of conventional measurement techniques. *Journal of Geophysical Research*, 112, D11307, <https://doi.org/10.1029/2006JD007971>

Stieb, D.M., Chen, L., Hystad, P., Beckerman, B.S., Jerrett, M., Tjepkema, M., Crouse, D.L., Omariba, D.W., Peters, P.A., van Donkelaar, A., Marin, R.V., Burnett, R.T., Liu, S., Smith-Doiron, M., Dugandzic, R.M. (2016). A national study of the association between traffic-related air pollution and adverse pregnancy outcomes in Canada, 1999–2008. *Environmental Research*, 148, 513–526. <https://doi.org/10.1016/j.envres.2016.04.025>

Tuzson, B., Zeyer, K., Steinbacher, M., McManus, J.B., Nelson, D.D., Zahniser, M.S., Emmenegger, L., (2013). Selective measurements of NO, NO<sub>2</sub> and NO<sub>y</sub> in the free troposphere using quantum cascade laser spectroscopy. *Atmospheric Measurement Techniques*, 6, 927–936. <https://doi.org/10.5194/amt-6-927-2013>

Villena, G., Bejan, I., Kurtenbach, R., Wiesen, P., Kleffmann, J. (2012). Interferences of commercial NO<sub>2</sub> instruments in the urban atmosphere are in a smog chamber. *Atmospheric Measurement Techniques*, 5, 149–159. <https://doi.org/10.5194/amt-5-149-2012>

Wada, R. and Orr-Ewing, A.J. (2005). Continuous wave cavity ring-down spectroscopy measurement of NO<sub>2</sub> mixing ratios in ambient air. *Analyst*, 130, 1595–1600. <https://doi.org/10.1039/b511115c>

WHO (2013). World Health Organization. *Review of evidence on health aspects of air pollution – REVIHAAP Project. Technical Report.* [http://euro.who.int/\\_data/assets/pdf\\_file/0004/193108/REVIHAAP-Final-technical-report.pdf](http://euro.who.int/_data/assets/pdf_file/0004/193108/REVIHAAP-Final-technical-report.pdf)

WMO-GAW (2017). World Meteorological Organization. *WMO Global Atmosphere Watch Implementation Plan: 2016–2023.* GAW Report No. 228. [https://library.wmo.int/doc\\_num.php?explnum\\_id=3395](https://library.wmo.int/doc_num.php?explnum_id=3395)